FOR ...

NOT TO BE TAKEN FROM THIS ROOM

HIGH VACUUM EVAPORATION, DEPOSITION MONITORING, & RATE CONTROL

by

Turgut Berat KARYOT

Submitted to the Faculty of the
school of Engineering in Partial Fulfillment
of the Requirements for the Degree of
MASTER OF SCIENCE
in
ELECTRICAL ENGINEERING

Boğaziçi University

September 1982

A C K N O W L E D G E M E N T

This thesis has been prepared for the partial fulfillment of the requirements of Bogazici University, School of Engineering for the degree of Master of Science in Electrical Engineering and been supported by Physics Department.

It is a pleasure to thank Dr.Naci Balkan, thesis supervisor, for his encouragement and guidance in the accomplishment.

A B S T R A C T

In order to determine the physical properties of amorphous semiconductor materials it is required to obtain thin film layers by high vacuum evaporation technique. Physical properties of such films are known to be strongly influenced by the rate of deposition.

This project therefore involves the construction of a thickness monitor and rate controller which monitors the thicness of thin film layers continuously during the evaporation process and keeps the evaporation rate constant at any desired value.

The change of thickness of the thin film layer is observed by monitoring the change in the oscillation frequency of a quartz crystal situated by the side of the thin film deposit.

All required functions are generated digitally.

Ö Z E T

Amorf Yarıiletkenlerin fiziksel özelliklerinin incelenmesi amacı ile yüksek vakumda buharlaştırma yöntemi ile ince filimler oluşturmak gerekmektedir. Bu filimlerin fiziksel özelliklerinin birikme hızından şiddetle etkilendiği bilinmektedir.

Dolayısı ile bu proje ince film tabakalarının kalınlığını buharlaşma işlemi sırasında sürekli olarak monitor eden ve buharlaşma hızını istenen herhangi bir değerde sabit tutan bir kalınlık monitoru ve hız kontrol devresinin yapılmasını içerir.

İzlenen ince film kalınlığının değişimi, filmin yanında yer alan bir kuartz kristalin titreşim frekansının değişimi yoluyla algılanmaktadır.

Tüm fonksiyonlar sayısal olarak üretilmektedir.

TABLE OF CONTENTS

ACKNOWLEDGEMENT
ABSTRACT
OZET
TABLE OF CONTENTS
PART A - VACUUM EVAPORATION TECHNIQUE

I - INTRODUCTION

II - THE CONSTRUCTION AND USE OF VAPOR SOURCES

III - THICKNESS DISTRIBUTION OF EVAPORATED FILMS

IV - DEPOSITION MONITORING AND CONTROL
A- Monitoring of the vapor stream
B- Monitoring of the deposited mass

PART B - THE DIGITAL APPROACH

I - INTRODUCTION

II - SYSTEM PRESENTATION

III - DEPOSITION MONITORING
A- Up/down frequency counter
1. Counter unit
2. Control unit
3. Time base unit
4. Display unit
B- Variable frequency oscillator

VI - EVAPORATION RATE CONTROL
A- Frequency rate control
1. Counter, control, time base units
2. Arithmetic logic and display units
B- Proportional or microprocessor compatible rate control unit
1. Phase locked loop and VCO units
2. Counter unit
3. Comparator unit
4. SCR trigger unit

Appendix 1: Power Unit

Appendix 2: General Configuration of the System

References

PART A

VACUUM EVAPORATION TECHNIQUE

PART A

VACUUM EVAPORATION TECHNIQUE

1. INTRODUCTION

The first evaporated thin films were probably the deposits which Faraday obtained in 1857 when he exploded metal wires in an inert atmosphere. Further experimentation in the ninteenth century was stimulated by interest in the optical phenomena associated with thin layers of materials and by investigations of the kinetics and diffusion of gases. The possibility of depositing thin metal films in a vacuum by Joule heating of platinum wires was discovered in 1887 by Nahworld and a year later adapted by Kundt for the purpose of measuring refractive indices of metal films. In the falloving decades, evaporated thin films have found industrial usage for an increasing number of purposes. Examples are antireflection coatings, front-surface mirrors, interferance filters, sunglasses, decorative coatings on plastics and textiles, in the manufacture of cathode ray tubes and most recently in electronic circuits.

Although commonly reffered to as a single process, the deposition of thin films by vacuum evaporation consists of several distinguishable steps:

i) Transition of a condensed phase, which may be solid or liquid, into the gaseous state.

ii) Vapor traversing the space between the evaporation source and the substrate at reduced gas pressure.

iii) Condensation of the vapor upon arrival on the substrates.

Accordingly, the theory of vacuum evaporation includes

the thermodynamics of phase transitions from which the equilibrium vapor pressure of materials can be derived, as well as the kinetic theory of gases which provides models of the atomistic processes.

Further investigations of the somtimes complex events occuring in the exchange of single molecules between a condensed phase and its vapor led to the theory of evaporation, a specialized extension of the Kinetic theory. From this basis the distribution of deposits on surfaces surrounding a vapor source can be derived.

Experimentally, vacuum evaporation and its applications have benefited from various disciplines which have contributed toward solutions of practical problems. These pertain to the construction of suitable vapor sources, the development of special techniques for the evaporation of alloys, compounds, and mixtures, and to questions of process control and automation.

II. THE CONSTRUCTION AND USE OF VAPOR SOURCES

The evaporation of materials in a vacuum system requires a vapour source to support the evaporant and to supply the heat of vaporization while maintaining the charge at a temperature sufficiently high to produce the desired vapor pressure. The rates utilized for film deposition may vary from less than 1 to more than 1000 Å per second, and the vaporization temperatures of any particular element differ accordingly. Rough estimates of source operating temperatures are commonly based on the assumption that vapor pressures of 10^{-2} torr must be established to produce useful film condensation rates. For most materials of practical interest, these temperature fall into the range from 1000 to 2000 °C.

To avoid the contamination of the deposit, the support material itself must have negligible vapor and dissociation pressures at the operating temperature. Suitable materials are refractory metals and oxides. Further selection within these categories is made by considering the possibilities of alloying and chemical reactions between the support and evaporant materials. Alloying is often accompanied by drastic lowering of the melting point and hence may lead to rapid destruction of the source. Chemical reactions involving compounds tend to produce volatile contaminants such as lower oxides which are incorporated into the film. Additional factors influencing the choice of support materials are their availability in the desired shape (wire,sheet,crucible) and their amenability to different modes of heating. The former determines the amount of evaporant which the source can hold (capacity), while the latter affects the complexity of the

source structure and the external power supply. Attempts to reconcile these demands have led to numerous source designs (1.). Specialized sources of rather complex constructions are nearly always required to evaporate quantities in excess of a few grams.

Principal types of evaporation sources are:

a) Wire and Metal foil sources.
b) Sublimation Sources.
c) Crucible Sources.
   its materials are:
   - Refractory metals.
   - Refractory oxides.
   - Boron nitride.
   - Carbon.
d) Electron-bombardment Heated Sources.
   its types are:
   - Work-accelerated Electron Guns.
   - Self-accelerated Electron Guns.
   - Bent-beam Electron Guns.

The simplest vapor sources are resistance-heated wires and metal foils of various types; as shown in Fig.1. They are commercially available in a variety of sizes and shapes at sufficiently low prices to be discarded after one experiment if necessary. Materials of construction are the refractory metals which have high melting points; and low vapor pressures. Most commonly used are tungsten, molybdenum and tantalum.

The sources shown in Fig.1a and b are commonly made from 0.02 to 0.06 in diameter tungsten wire. Their utility is limited to evaporants which can be affixed to the source,

typically in the form of wire. Upon melting, the evaporant must wet the filament and be held by its surface tension. Spreading of the molten evaporant across the wire is desireable to increase the evaporation surface and thermal contact. Multistrand filaments where the evaporant is added as one of the fibers is a suitable technique.

Multistrand filaments are generally preferred because they offer a greater surface area than single filaments.

Wire baskets as shown in Fig.1c are used to evaporate pellets or chips of dielectrics or metals which either sublimate or do not wet the wire material upon melting.

Metal foils as shown in Fig.1d,e,f have capacities of a few grams and are the most universal types of sources for small evaporant quantities. They are fabricated from 0.005-0.015 in thick sheets of tungsten, molibdenum or tantalum. They have reduced widths in the center to concentrate the heating in the area of evaporant.

Electrical connections to wire and foil sources are made by attaching their ends to heavy copper or stainless-steel clamps. The latter are usually part of massive metal bars connected rigidly to a pair of electrical feedthroughs. Since the electrical resistance of wire and foil sources are small, low voltage power supplies rated 1 to 3 KW are required. Typical arrangements consists of a step down transformer, 220 to 20 volts. The secondary current may be as low as 20 A for some of the wire sources, or as high as 500A for some foil sources. Whenever the current exceeds 100A, the feedthroughs are water cooled.

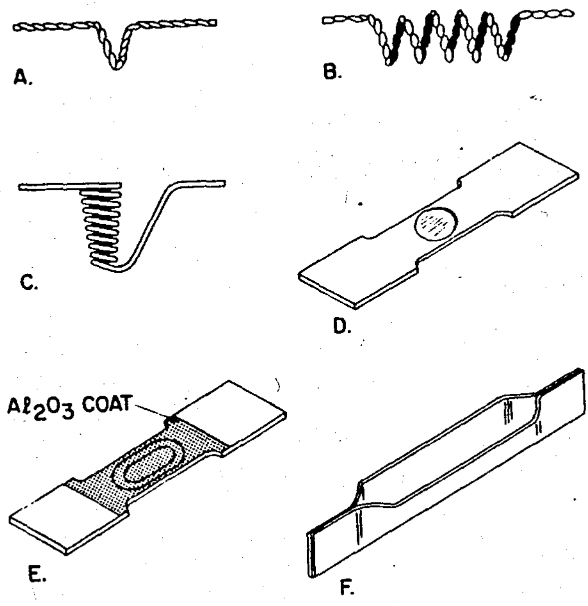

Fig.1

Wire and metal foil sources

A) Hairpin Source

B) Wire Helix

C) Wire Basket

D) Dimpled Foil

E) Dimpled foil with alumina coating

F) Canoe type

III. THICKNESS DISTRIBUTION OF EVAPORATED FILMS

Since most practical applications require a certain film thickness, the substrate area which can be covered uniformly is a significant figure of merit for vapor sources. The distribution of deposits can be derived as follows:

An isothermal enclosure with an infinitesimally small openning dA_e bounded by vanishingly thin walls is shown schematically in Fig.2.

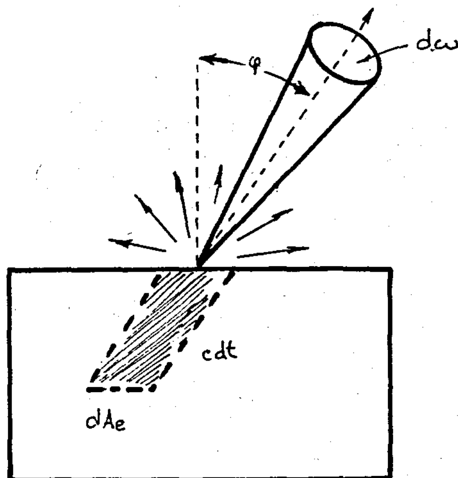

Fig.2

Effusion from an isothermal enclosure through a small orifice.

It is assumed to have N molecules which have a Maxvellian speed distribution. Most of these molecules will impinge on the enclosure walls and be reflected without causing a net change in the total speed distribution. Considering first molecules of only one particular speed c, their total number in the enclosure is $dN_c=N\phi(c^2)dc$. Within a time dt, only those molecules can reach dA_e and leave in the direction which are in the slanted prism. Thus the fraction of molecules within striking distance of the opening is $c.dt.\cos\varphi.dA_e/V$. The number of molecules actually

crossing the opening is further reduced because their speeds c within the slanted prism are randomly distributed in all directions. Hence only the fraction $dw/4$ is actually moving toward dA_e. Multiplication of dN_c with the volume fraction and the angular fraction yields the number of molecules having a speed c and leaving in the direction :

$$d^4.N_{e,c}(\varphi)= \frac{N}{V}.c.\phi(c^2).dc.dA_e.dt.\cos\varphi.\frac{dw}{4\pi} \qquad \text{(eq.1)}$$

Integration over all speeds c gives the total number of molecules per angle increment dw, whereby

$$\int_0^\infty c\phi(c^2)\ dc= \bar{c} \qquad \text{(eq.2)}$$

and therefore

$$d^3.N_e(\varphi)= \tfrac{1}{4}\,\frac{N}{V}.\bar{c}.dA_e.dt.\cos\varphi.\frac{dw}{\pi} \qquad \text{(eq.3)}$$

The small increment of mass carried by these molecules is

$$d^3.M_e(\varphi)=m.d^3.N_c(\varphi) \qquad \text{(eq.4)}$$

let $\Gamma=m.\frac{1}{4}.(N/V).\bar{c}$ one obtains (eq.5)

$$d^3.M_e(\varphi)= \Gamma.dA_e.dt.\cos\varphi\,\frac{dw}{\pi} \qquad \text{(eq.6)}$$

$$M_e=\int_t\int_{A_e}\Gamma.dA_e.dt \qquad \text{(eq.7)}$$

$$dM_e(\varphi)= M_e.\cos\varphi.\frac{dw}{\pi} \qquad \text{(eq.8)}$$

According to this cosine law, emission of material

from a small evaporating area does not occur uniformly in all directions but favors directions approximately normal to the emitting surface where cos φ has its maximum values.

The amount of material which condenses on an opposing surface also depends on the position of the receiving surface with regard to the emission source. As shown in Fig.3, the material contained in an evaporant beam of solid angle dw covers an area which increases with distance as well as with the angle of incidence θ. The element of the receiving surface which corresponds to dw is $dA_r = r^2 . dw/\cos\theta$. Therefore the mass deposited per unit area is

$$\frac{dM_r(\varphi,\theta)}{dA_r} = \frac{M_e}{\pi r^2} . \cos\varphi . \cos\theta \qquad \text{(eq.9)}$$

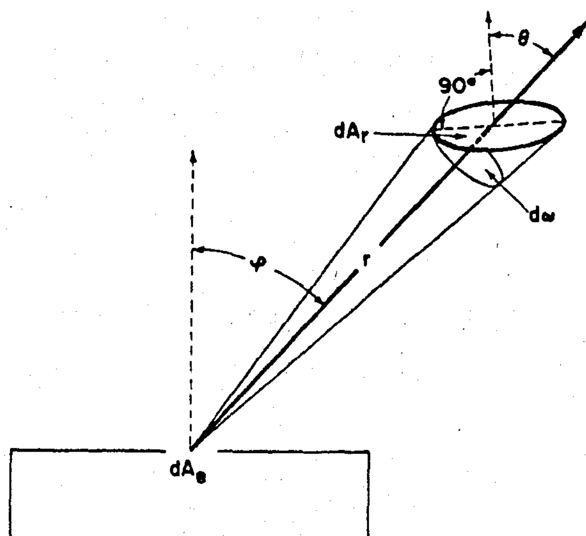

Fig.3

Surface element dA_r receving deposit from a small area source dA_e.

If a point evaporation source is admitted, the mass evaporation rate will be uniform in all directions, and the mass contained in a narrow beam of solid angle dw will be

$$d^3.M_e = \Gamma.dA_e.dt.\frac{dw}{4\pi} \qquad \text{(eq.10)}$$

Since $\int_t \int_{A_e} \Gamma.dA_e.dt$ is the total evaporated mass M_e,

$$dM_e = M_e.\frac{dw}{4\pi} \qquad \text{(eq.11)}$$

For a receiving element dA_r, within the solid angle dw, the dependence on source distance and beam direction is the same as for a small surface source, $dA_r = r^2.dw/\cos\theta$, and therefore the amount of deposit received from a point source is

$$\frac{dM_r}{dA_r} = \frac{M_e}{4\pi r^2}\cos\theta \qquad \text{(eq.12)}$$

The receiving element of uniform deposit is thus a sphere with the point source in the center so that $\cos\theta=1$ and $r=C^{st}$.

These above expressions represent the idealized behaviour. In practice however, it is found that the emission patterns of many useful sources deviate from the idealized behaviour. The causes of such modified emission patterns are collisions of evaporated molecules among each other and with the walls constituting part of the source. The mathematical formulation of modified emission laws has often been attempted but is difficult, and the resulting expressions apply only to effusion cells with well-defined orifices.

Normally, the substrates are planar and parallel to the plane of the emitting surface. The mass received at a point on the substrate defined in terms of r, φ, θ is given

by equations 9 and 12. To convert mass into film thickness d, one may visualize the small mass dM_r occupying a volume of $dA_r.d$. If ϱ is the density of the film material, then

$$d = \frac{1}{\varrho} \cdot \frac{dM_r}{dA_r} \qquad \text{(eq.13)}$$

For a plane-parallel receiver at a distance h from the source, the angle of incidence θ equals the emission angle φ, $\cos\phi = \cos\theta = h/r$.

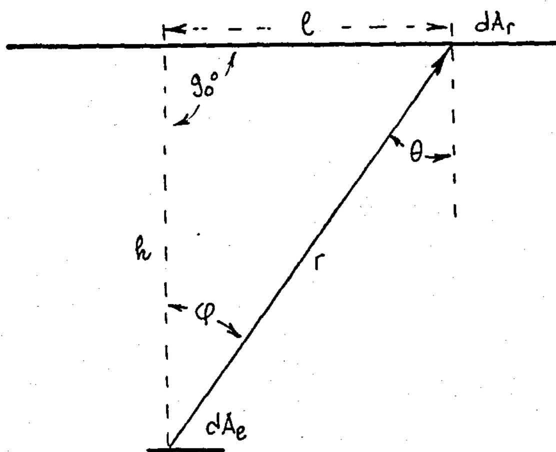

Fig.4

Evaporation onto a plane parallel receiver.

The evaporation distance r for surface element dA_r varies with the distance ℓ from the center of the substrate area according to $r^2 = h^2 + \ell^2$. Substituting these relations into eqs. 9,12,13 we get

For small area source: $$d = \frac{M_e}{\pi \varrho h^2 (1+(\ell/h)^2)^2} \qquad \text{(eq.14)}$$

For the point source: $$d = \frac{M_e}{4\pi \varrho h^2 (1+(\ell/h)^2)^{3/2}} \qquad \text{(eq.15)}$$

Since both sources have infinitesimally small evapora-

tion areas dA_e, the evaporated mass M_e, and hence d, too, are differential quantities. Without assuming that eqs. 9 and 12 also apply for small but finite areas, the emission characteristics of the two source types may be defined in terms of the ratio d/d_o, where d_o is the center thickness at l=o. This leads to

For small area source: $$\frac{d}{d_o} = \left[1+\left(\frac{\ell}{h}\right)^2\right]^{-2} \quad \text{(eq.16)}$$

For the point source: $$\frac{d}{d_o} = \left[1+\left(\frac{\ell}{h}\right)^2\right]^{-3/2} \quad \text{(eq.17)}$$

IV. DEPOSITION MONITORING AND CONTROL

The objective in vacuum evaporation is nearly always to obtain films to certain specifications. If the latter pertain to film properties which are primarily extensive such as thickness or sheet resistance it is sufficient to determine when the accumulated deposit has reached the desired value so that the process can be terminated. However intensive film properties such as density, resistivity, stress or crystallinity depend on the rates at which evaporant and residual gas molecules arrive at the substrate. It is therefore often necessary to maintain specified evaporation rates. The sensing devices which allow measurements during the evaporation process are referred to as either thickness or rate monitors. They exploit different physical effects to determine the density of the evaporant stream, the mass of the deposit, or a thickness-dependent film property.

Traditionally, monitoring devices have been constructed by individual investigations to suit their particular purpose. Several types of monitors have become commercially available during the last few years. Reviews of thickness and rate monitors have been given by Steckelmacher(2) and Behrndt(3).

a) Monitoring of the vapor stream.

There are two methods of measuring the density of the evaporant stream.

- Ionization-Gauge rate monitors: The vapor molecules

are ionized by collisions with electrons, and the ions are collected.

- Particle-impingment rate monitors: It is based on measuring the dynamic force which impinging particles exert on a surface.

b) Monitoring of the deposited mass.

Mass sensing devices may be used for all evaporant materials. They operate either by determining the weight of the deposit, or by detecting the change in oscillating frequency of a small quartz crystal on which the evaporant condenses.

i) Microbalances: Instruments suitable for the gravimetric determination of small quantities of mass. Their design may be based on different principles such as the elongation of a thin quartz-fiber helix, the torsion of a wire, or the deflexion of a pivot mounted beam(4).

ii) Crystal oscillators: The use of crystal oscillators to determine small quantities of deposited matter was first explored by Sauerbrey(5-6) and Lostis(7). The transducers required to monitor film thickness are of relatively simple construction and about as sensitive as microbalances while practically unaffected by mechanical shocks and external vibrations.

Therefore crystal oscillators have recieved much interest during the last years and are currently the most widely used means for monitoring film depositions. The crystal oscillator monitor utilizes the piezo-electric properties of quartz. A thin crystal wafer is contacted on its two surfaces and made part of an oscillator circuit.

The ac field induces thickness-shear oscillations in the crystal whose resonance frequency is inversely proportional to the wafer thickness d_q,

$$f = \frac{C_t}{2d_q} \qquad \text{(eq.18)}$$

where C_t is the propagation velocity of the elastic wave in the direction of thickness. The major surfaces of the wafer are antinodal.

An important consideration in preparing the quartz wafer is the temperature dependence of the resonance frequency. The temperature coefficient of frequency (TCF) of quartz is related to the elastic constants. It has positive and negative terms whose magnitudes depend on the direction of the vibration with respect to the natural crystal axes. Since frequency changes resulting from temperature fluctuations affected the accuracy of mass determinations, the quartz crystals are cut in an orientation where the TCF terms compensate each other. The orientation is designed as an AT cut and is used in all thickness monitors. The temperature dependence of the TCF for a number of AT crystals of slightly different orientation has been measured by Phelps (8). Fig.5 shows the function for a cut made at $35^\circ 20'$. The TCF reaches zero at about $30^\circ C$ and remains smaller than $\pm 5.10^{-6}$/deg in a temperature interval of about $\pm 30^\circ C$. Changes in the cutting angle of only 10' shift the temperature of zero TCF by as much as $50^\circ C$ and also narrow the interval of small TCF values.

The cutting angles generally preferred are between $35^\circ 10'$ and $35^\circ 20'$. The resonance frequencies for thickness-shear mode oscillations of AT crystals are given by

$$f_o = \frac{N}{d_q} \qquad \text{(eq.19)}$$

where N≐ 1.67×10^6 Hz mm.

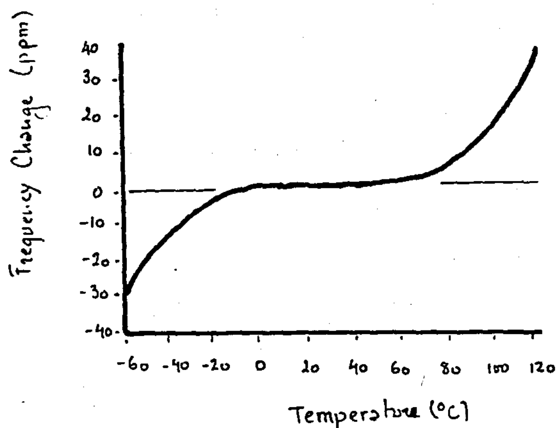

Fig.5

Frequency change vs. temperature for an AT crystal cut at $35^o20'$

If a small M is added to either one or both sides of the wafer, it may be assumed that the original crystal surfaces remain antinodes of vibration. Hence the deposit affects the resonance frequency only through its mass whereas material specific properties such as density or elastic constants are inconsequential. The effect of mass loading on the frequency may be derived by differentiating eq.19 with respect to d_q and substituting the added increment of quartz Δd_q by an identical mass ΔM of foreign matter and different thickness d_f(6). An alternative derivation was given by Stockbridge(9) who applied perturbation analysis to a resonating plate and obtained essentially the same relation:

$$\Delta f = -\frac{K f_o^2}{N \rho_q} \frac{\Delta M}{A_m} = -\frac{K N}{\rho_q d_q^2} \frac{\Delta M}{A_m} \qquad \text{(eq.20)}$$

where ρ_q is the density of quartz($2.65 gr/cm^3$), K=1 is a constant which depends on the distribution of deposit over the monitor area A_m. The latter should be the total surface area of the wafer. However, if the electrodes applied to the wafer cover only part of the crystal surface, as is often

the case, then A_m is to be taken as the electrode area. It has been shown that oscillations outside the electrode area are negligible and deposits there contribute only 1% to the frequency change Δf (6).

The proportionality factor in eq.20 is called the mass determination sensitivity of the crystal.

$$C_f = \frac{f_o^2}{N \rho_q} = \frac{N}{\rho_q d_q^2} \quad \text{Hz cm}^2/\text{gr.} \qquad \text{(eq.21)}$$

As shown in Fig.6 the thinner crystals with the higher resonance frequencies give larger frequency changes per deposited mass per unit area.

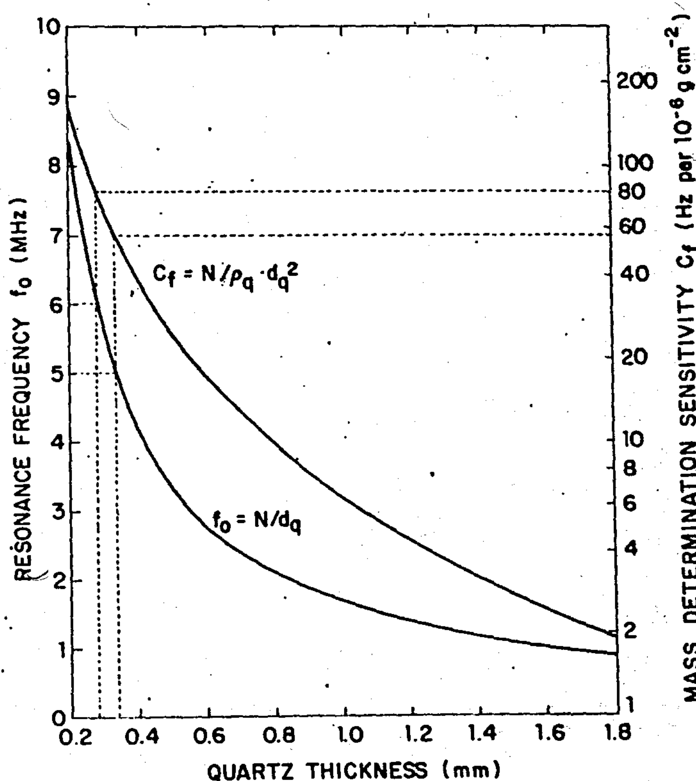

Fig.6

Resonance frequency and mass-determination sensitivity of AT crystals as function of wafer thickness.

Hence, in the interest of sensitivity, the crystal

wafers should be made as thin as their fragility permits. There is however, another limitation. The relationship between Δf and ΔM ceases to be linear if the thickness of the deposited mass is no longer small compared with the wafer thickness. Estimates as to how far linearity may be assumed without committing significant errors vary from Δf_{max}=0.5% (3) to 5% (2) of the initial frequency f_o. Althoug the maximum permissible frequency change is larger for the thinner crystals, the mass which causes this Δf_{max} is greater for the less sensitive (thicker) crystals, as shown in Fig.7.

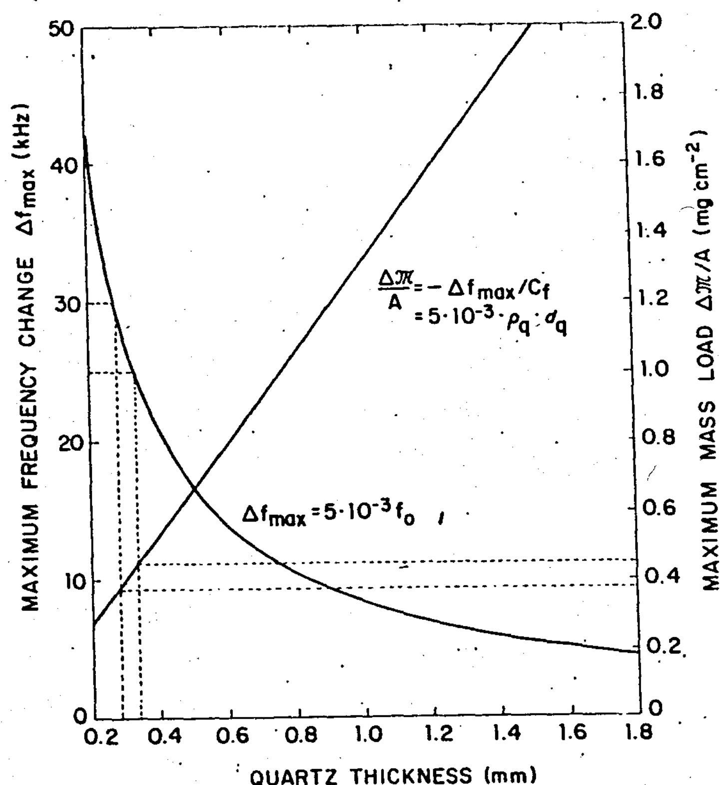

Fig.7

Maximum frequency change and mass loading for AT crystals as function of wafer thickness.

Crystals of about 0.3 mm thickness with initial frequencies of 5 to 6 MHz are generally considered to offer the best compromise between high sensitivity and high mass loading capacity.

The mass frequency equation 20 has repeatedly been

verified by control experiments with microbalances. Eschbach and Kruidhof (10) obtained an experimental value of C_f which agreed within 0.4% with the value derived from the material parameters of quartz. It is therefore not necessary to calibrate monitor wafers empirically, but the temperature of the crystal should be taken into account. Empirical values of f_{max} for 5MHz crystals range from 50 to 100 KHz, which is equivalent to deposits of 1 to 2 mg/cm^2 (10,11,12). The corresponding maximum thickness

$$d = \frac{\Delta M \cdot 10^8}{\rho A_m} \text{ Å} \qquad \text{(eq.22)}$$

varies from 5000 to 50.000 Å depending on the density of the film material.

The crystals used in deposition monitors are either circular or square platelets of typically 13-14 mm size. They are mounted in holders which prevent them from shifting position, yet allow easy removal and replacement.

Although AT cut wafers have the smallest possible temperature coefficient of frequency, it is still necessary to protect the crystal against temperature changes due to radiation from the source and heat of condensation. Therefore the crystal housing is usually water cooled and forms a radiation shield which surrounds the entire crystal except for the deposition area. The heat received by this necessarily exposed area still causes temperature increases of several degrees with ensuring frequency changes of 10 to 100 Hz.(11,12,13); which are equivalent to mass changes of 10^{-7} to 10^{-6} gr/cm^2. The effect can be minimized by using a small entrance aperture but is not negligible when making precision measurements.

Classically, the instrumentation required to operate a monitor consists basically of an oscillator and a suitable frequency meter. The common practice is to use a reference oscillator, with a fixed frequency and to generate a difference frequency. The latter is mixed again with the signal from a variable frequency generator as shown in Fig.8. The advantage of this arrangement is that it permits operation in the most sensitive frequency range regardless of the film thickness accumulated on the crystal. The output signal is in the audio-frequency range and drives the counter circuit.

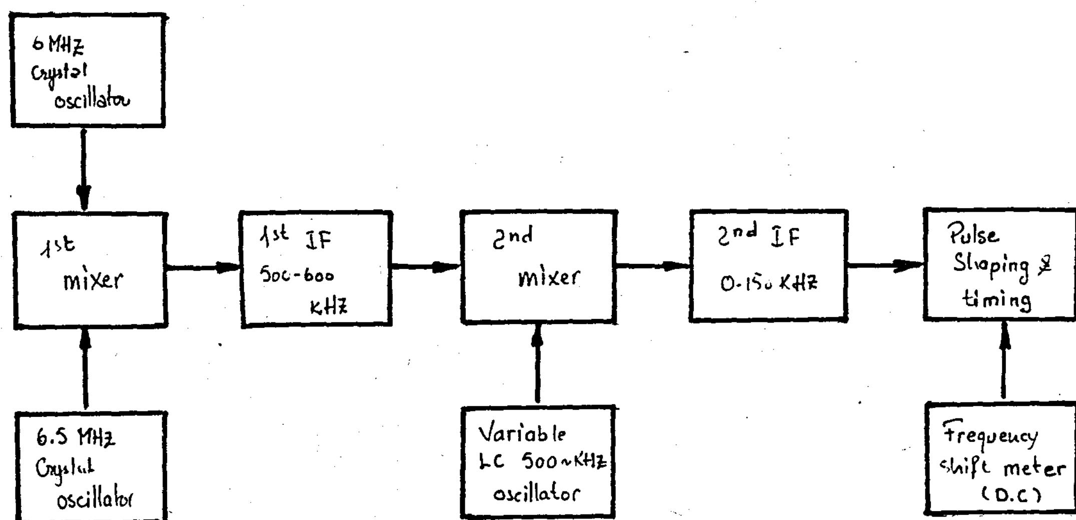

Fig.8 Block diagram of a typical film thickness monitor.

In practice, the accuracy of crystal oscillator monitor is determined by the stability of the oscillator

BOĞAZİÇİ ÜNİVERSİTESİ KÜTÜPHANESİ

circuit. If a frequency change of 1Hz in a 5MHz oscillator can be detected, the corresponding sensitivity is about $2 \cdot 10^{-8} gr/cm^2$.

Ordinarily, the stability of classical circuits is only of the order of 10 to 100 Hz/h. Thus the practical mass detection limit is 10^{-7} to 10^{-6} gr/cm^2 (14).

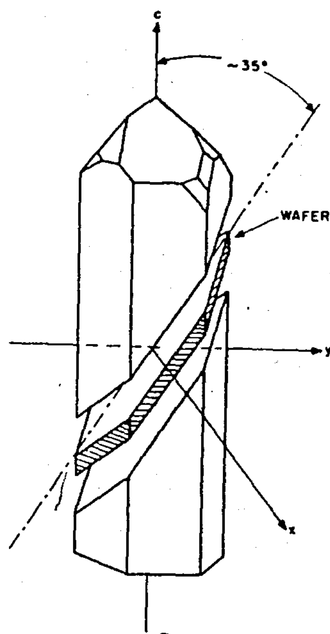

Fig.9 Quartz Crystal with AT cut wafer

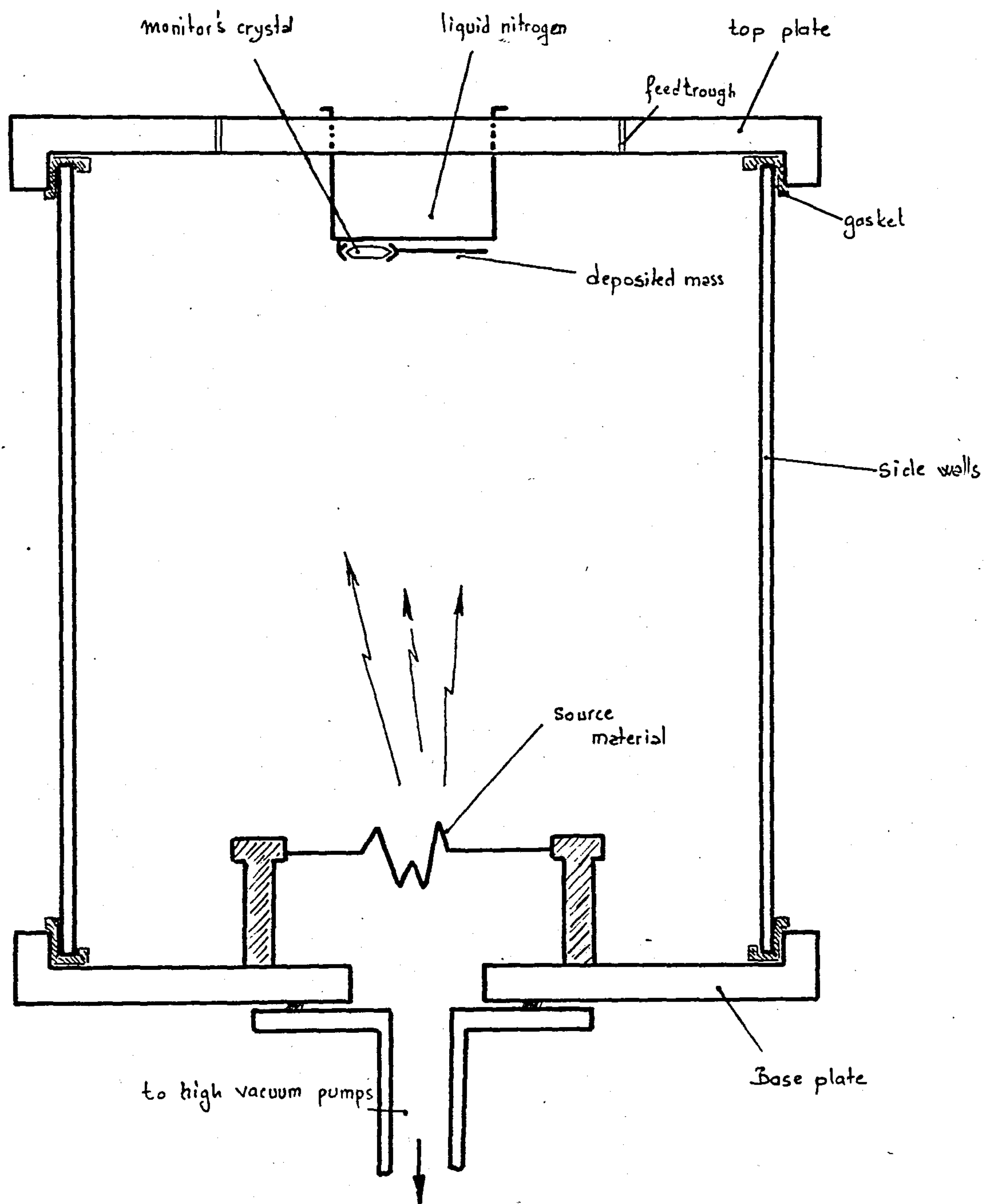

Fig.10 The vacuum chamber arrangement

PART B

THE DIGITAL APPROACH

PART B

THE DIGITAL APPROACH

1. INTRODUCTION

In crystal thickness monitors and rate controllers, a quartz crystal forms a part of the resonant circuit of a crystal controlled oscillator. The change in frequency of this oscillator due to the deposition on the crystal is usually measured by measuring the change in the frequency between this oscillator, and a second, reference oscillator. The change in beat frequency is detected quantitatively and manipulated to display the deposit thickness directly. But two difficulties are experienced with this type of monitor.

Since the difference between two oscillators is the quantity measured, the reference oscillator must be stable enough to introduce negligible error in the difference measurement. As the difference frequency is usually small compared to the oscillator frequency, this places strict requirements on the oscillator stability. Furthermore, it is desirable to set the output of the monitor to "zero" at the start of a deposition; and this is often done by adjusting the reference oscillator frequency. As the crystal oscillator frequency becomes progresively less with successive vapor depositions, this frequency maching becomes increasingly difficult to achieve by simple means, while maintaining reference oscillator stability.

In the system proposed, a reference oscillator was eliminated by the use of a resettable frequency memory. Elaborate beating and filtering methods were avoided by a straightforward digital subtraction of frequencies. No fur-

ther calibration or manipulation was necessary to read the change in frequency. The integrated circuits used in the monitor and rate controller were commonly available in the market. The frequency of the quartz crystal oscillator could be ready at any time, and hence the frequency could be followed as successive films were deposited. Furthermore the system being completely digital, the rate control unit can be operated in connection to a microprocessor for more sophisticated control systems, as well as it can function independently.

II. SYSTEM PRESENTATION

The blok diagram of the proposed system is given in Fig.1 . It mainly consists of two parts:

- deposition monitoring
- evaporation rate control

Deposition monitoring is based on the idea of measuring the actual frequency of the monitoring oscillator directly with a digital frequency meter and then subtracting it from the initial frequency in order to get the frequency difference, to determine the thickness of the deposited material. The final value is then displayed up to seven digits. This process ia renewed at every two seconds.

Evaporation rate control is based on taking the difference of two consecutive samples of change in frequency within 1, 10, 100 or 1000 seconds and then subtracting it from the required value or the set value. The error signal thus generated will then be used to trigger the triac which controls the rate of the evaporator source. The phase locked loop and voltage controlled oscillator is added to the triggering circuit in order to provide coherent operation of the triac with the mains.

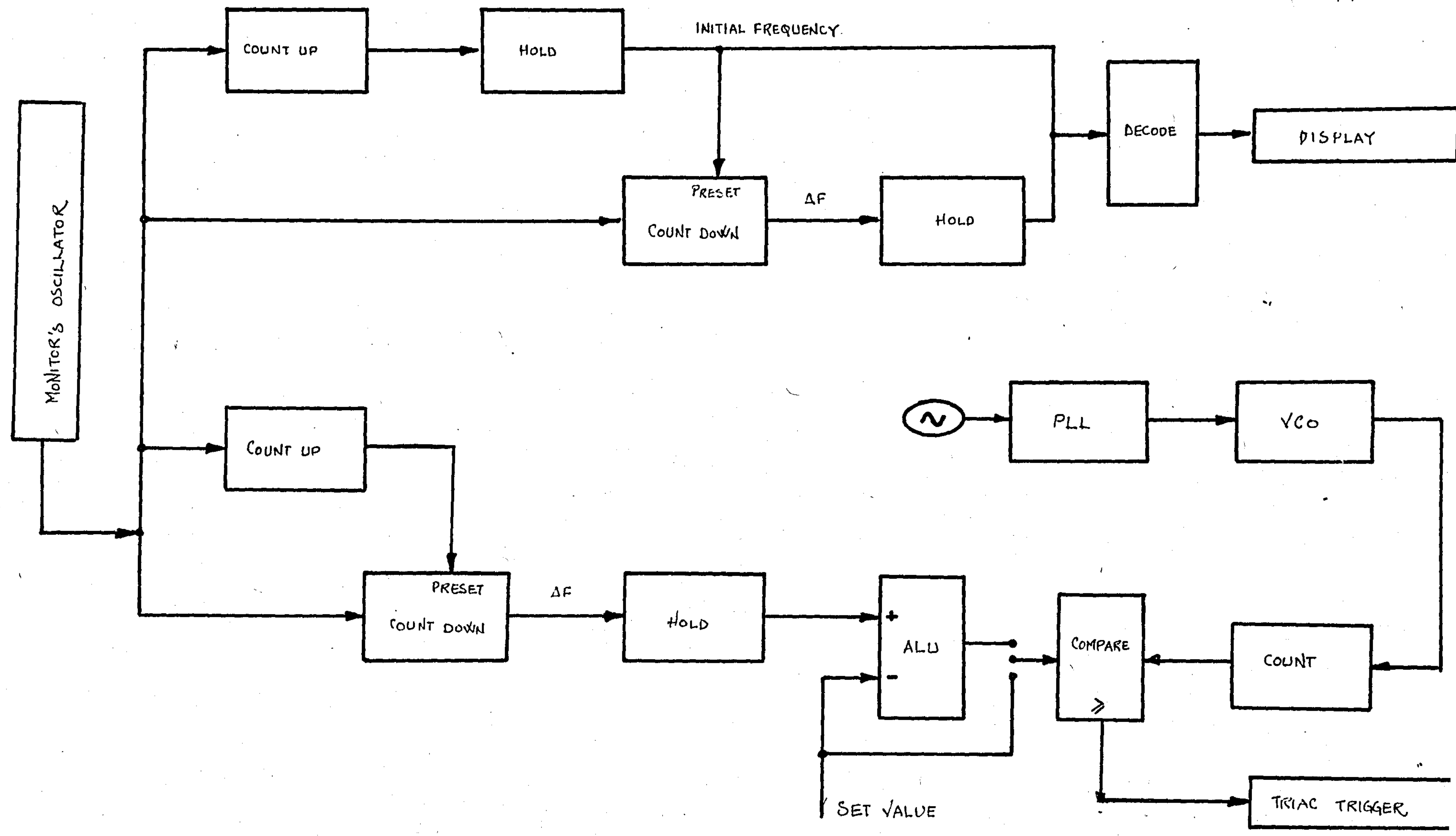

Fig.1

III. DEPOSITION MONITORING

The deposition is monitored via the change in frequency on an external oscillator (variable frequency oscillator). The data obtained is a seven digit frequency difference.

The block diagram of deposition monitoring system is given in Fig.2.

The system consists of two parts.

A- Up/Down frequency counter
B- Variable frequency oscillator

A - UP/DOWN FREQUENCY COUNTER

The frequency counter is the main part of the system. The deposited mass is monitored through this counter. It consists of four units. Counter, control, time base and display units.

Time base provides the reference timing for the functioning of all units. The control unit generates the neces - sary signals to the counter. The actual frequency or the change in frequency is then displayed to outside world in seven digit form via the display unit.

The circuit is as shown below.

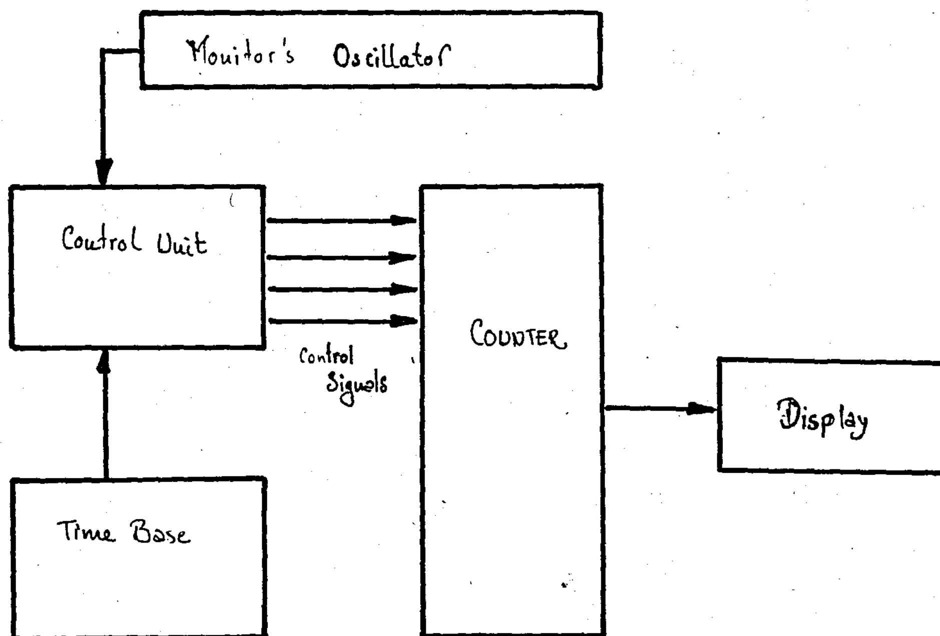

Fig.2

i- Counter Unit:

This unit is based on two integrated circuit chips 74192, presettable BCD decade up/down counter and 7475 four bit transparent latch used as temporary registers. 74192 being a four bit BCD up/down counter contains four master/slave flip-flops with internal gating and steering logic to provide asynchronous Master Reset and Parallel Load, and Synchronous Count up and Count down operations.

As shown in the Fig.3 the outputs of the 74192 are connected to data inputs of 1st 7475 group.

The 7475 when enabled the information present at its data inputs is transferred to its outputs and the information present is stored in the latch when the enable signal is removed. The output of the 1st group of 7475 is fed both to the data inputs of a 2nd group of 7475 and the 7448's the decoder driver chips of the display unit. The 2nd 7475 group functions as a memory unit, containing the same information during the hole evaporation process while the 1st 7475 group renews its information at each step of counting i.e. 2 secs.

Referring to Fig.4 the functioning of this unit is as follows. During the one second gating interval, output of the variable frequency oscillator is fed to Count Up pin of the 74192 to count the actual frequency. At the end of this interval the control unit sends a signal enabling 1st and then the 2nd 7475 latch groups. Accordingly, the counted frequency is fed to display drivers to be displayed on 7 digits, and is stored in the second group of latches. Then the Master reset pulse clears the content of the counter while the displayed information remains as it is. Just one second after the end of counting, a new sequence of counting starts. If the evaporation process have not occured,

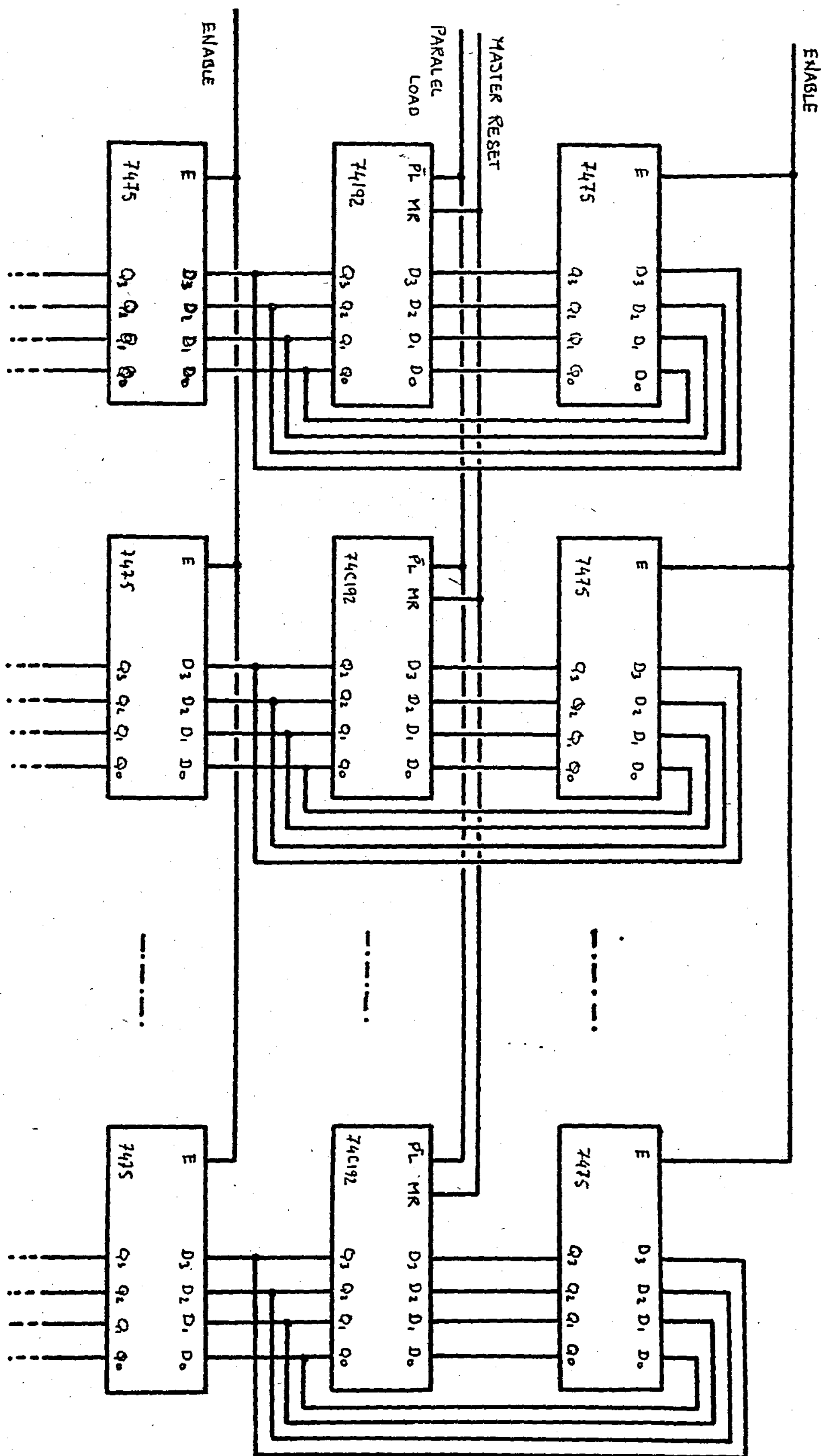

Fig.3

not occured, i.e. the frequency of the external oscillator did not change, the counter will count for the same number of times and consequently the display will show the same information. This process renewing the information in the 2nd group of latches provides calibrating of the monitor. Before starting the evaporation, the counter should be taken in count down mode. This is done by pressing the "actual frequency-decrease in frequency" button. The 74192 will now function in count down mode. The initial frequency counted and stored in 2nd group of 7475's during count up or calibrate modeis now transferred to 74192 by signaling its Parallel Load pin. The data present at the output of the 2nd group of latches is now transferred to the outputs of the counter chips and it will count now downwards during the same interval of 1 sec. If the external oscillator frequency did not changed, i.e. no deposition occured, the final display will be zero. If deposition occurred, due to the decrease in frequency of the oscillator circuit, the counter will count less than the initial calibrating frequency, and the difference will remain in the counter at the end of counting interval, thus that data will be displayed. In count down mode the 2nd group of latches are never enabled, so that the initial frequency is kept in the memory till the end of the evaporation process,in order to be used, parallel loading the 74192 at every 2 seconds. Once the count down mode is activated it proceeds till the end of the evaporation, displaying at every 2 seconds the difference between the initial and the actual frequency.

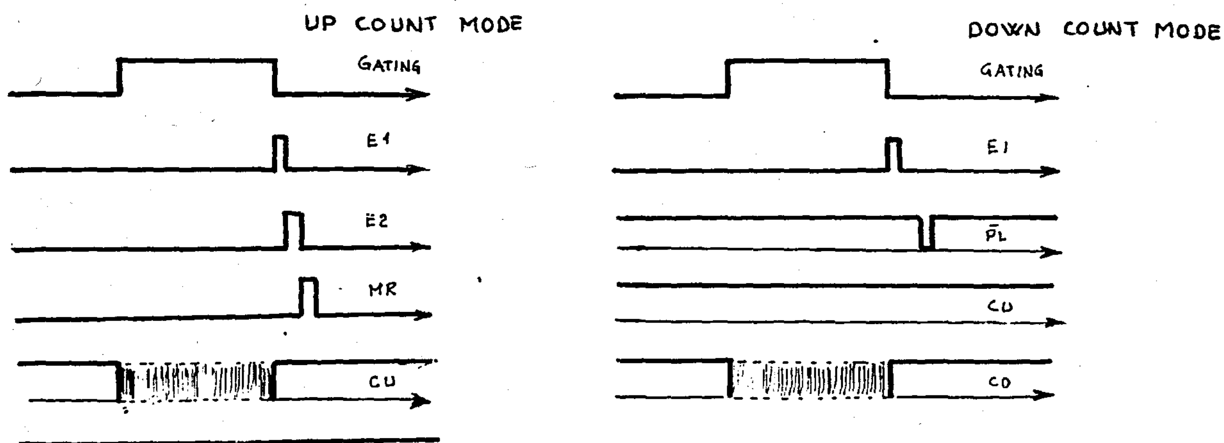

ii- Control Unit:

This unit is based on 7473 Dual JK flip-flop, 74123 Dual Monostable Multivibrator and 7400 quad nand gate chips to provide the control signals, namely: Count Up, Count Down, Parallel Load, Clear, Enable Latch for the counter unit, The circuit is shown in Fig. 5.

The first flip-flop works in toggle mode. The 1 sec clock input produces precisely a square pulse of 2 secs period. The 1 second long 1 level interval counting operation is performed by the counters. According to the switch position the Q and $\bar{Q}$ outputs of the second flip-flop are nanded with the oscillator and with the output of the 1st flip-flop produce count up or count down pulses. The circuit is so arranged that while one count is counting the other is in high logic.

The falling edge of the square pulse produced by the 1st flip-flop triggers a chain of monostable multivibrator. Just at the end of up counting both group of latches are enabled and the counters are then cleared by the clear pulse. If the unit is in count down mode, only the first enable and parallel load signals are produced.

The resistor and capacitor values for the monostable multivibrators are so chosen that the timing pulses obey to the specifications of the chips.

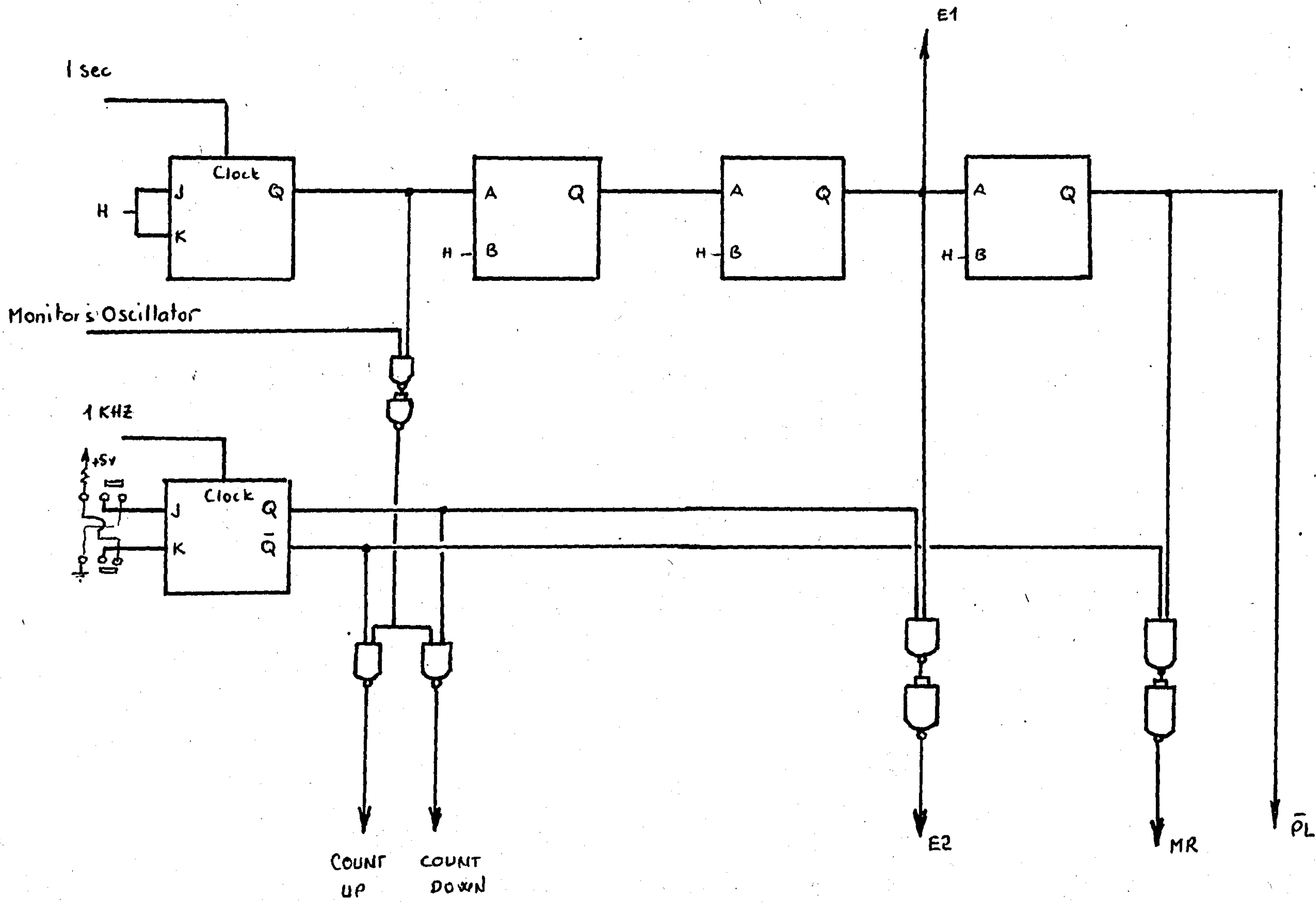

Fig.5 The control unit

iii- Time Base

This unit is the reference point of the counter. It consists of a crystal controlled astable multivibrator and a chain of BCD counters.

As shown in the Fig. 6 the N1 and N2 nand gates form the astable multivibrator, the frequency of which is controlled by the 100 MHz Quartz Crystal. This oscillator circuit has to be very stable and accurate because all the measuremants that we have made were based on its frequency. The other two nand gates N3 and N4 are used to amplify and shape the oscillator output to a clear square wave. This square wave of frequency equal to the one of the quartz, i.e. 1.0 MHz, is then divided by 10 several times in order to get 100 KHz, 10 KHz, 1 KHz, 100 Hz, 10 Hz and finally 1 Hz.

7490, the 4 bit ripple type decade counter is best suited for this dividing process. It has two sections providing divide by two and divide by 5 functions. To obtain divide by 10, the divide by 2 output is externally connected to divide by 5 input.

Vcc

R1 R3 N1 N2 N3 N4 7400 C2 C3 X-tall 1MHZ R2 R4 C1

GND MS MR Q0 CP1 Q3 $\overline{CP_0}$ Vcc

1HZ 10HZ 1KHZ

Fig.6 The time base

iv- Display unit

This unit is based on the 7448 BCD to seven-segment decoder driver. It accepts four bit BCD input and produces appropriate outputs for selection of segments in a seven-segment matrix display used for representing the decimal number "0-9". The seven outputs a,b,c,d,e,f,g of the decoder select the corresponding segments in the matrix as shown below.

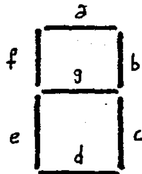

Fig. 7

The connection diagram is shown below.

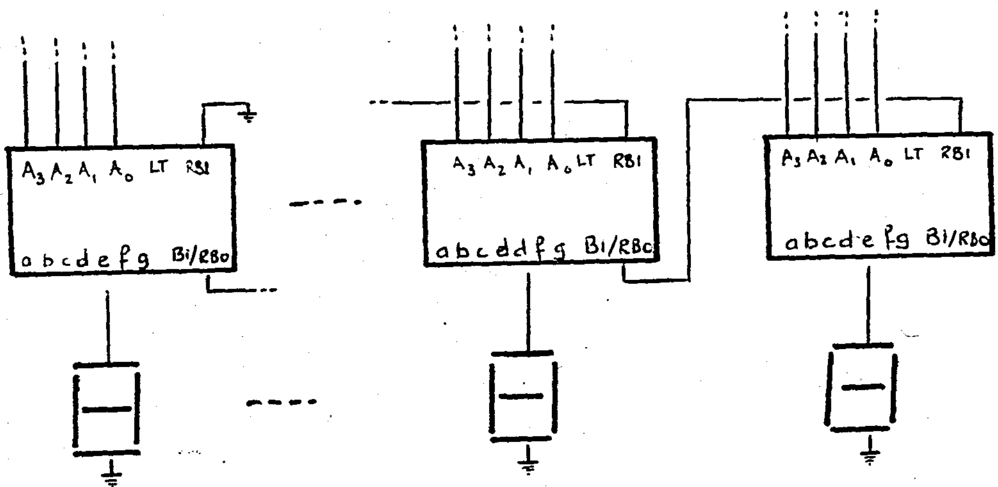

Fig. 8

B - VARIABLE FREQUENCY OSCILLATOR

The monitoring crystal forms the heart of this oscillator. The evaporated material deposited on the crystal, causes a shift in its frequency thus, of the oscillator.

Physically the monitor oscillator should be as compact as possible in order to be installed into the vacuum chamber.

The electronic circuit of the variable frequency oscillator is just like the oscillator circuit of the time base circuit. The frequency of the astable multivibrator is controlled by the quartz crystal.

The circuit is shown below.

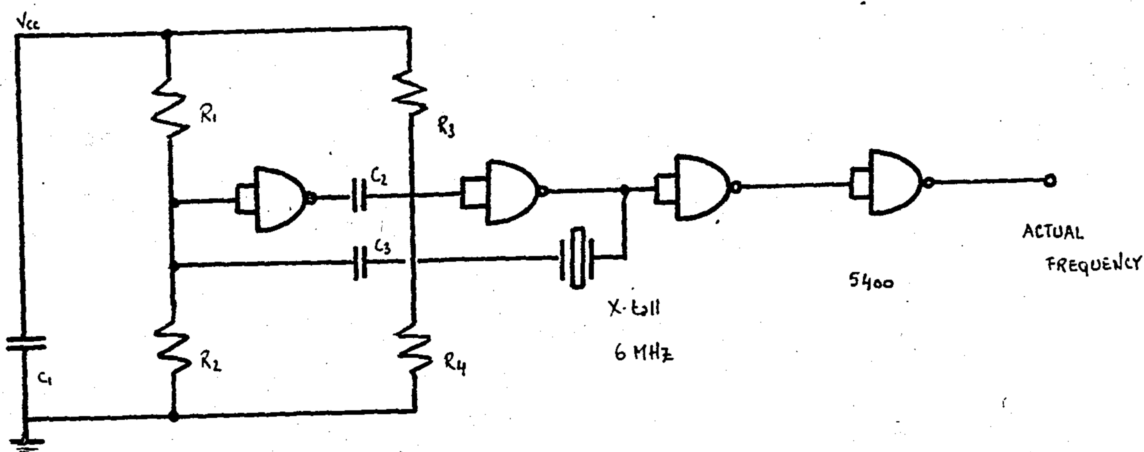

Fig.9

IV. EVAPORATION RATE CONTROL

Once evaporation is started, generally it is required to have a constant amount of material evaporated and deposited during constant intervals of time. Therefore it is worthy to monitor the changes in decrease of the frequency. This decrease of the frequency in a certain amount of time interval can be desired to have some different levels for different evaporant material and also for different experimental purposes. A set value input is then needed to provide to the system the required level.

The evaporation rate controller consists basically of a "change in the rate of the frequency change" detector and a suitably varying evaporator's supply unit.

The system is designed in such a way that, the evaporation rate can be controlled for 0 up to 255 Hz decrease of frequency within 1-10-100 or 1000 second intervals. The system can be locked at any value between 0-255 Hz per time interval, and continues the process from there on.

0-255 Hz data is inputed to the system in binary form either by schitches or by interfacing to a microprocessor, programmed accordingly. The time interval is selected from a group of push-botton on the panel of the system.

A - FREQUENCY CHANGE DETECTOR

This detector used for rate control of the evaporator consists mainly of four units. Counter, control, error display and Arithmetic Logic Unit.

The counter unit counts the difference in frequency for the selected time interval. Arithmetic Logic Unit takes the difference between this actual value and the required value generating an error signal. This error is displayed in eight bit binary form. All timing and control signals for the proper functioning of this frequency change detector is generated by the control unit.

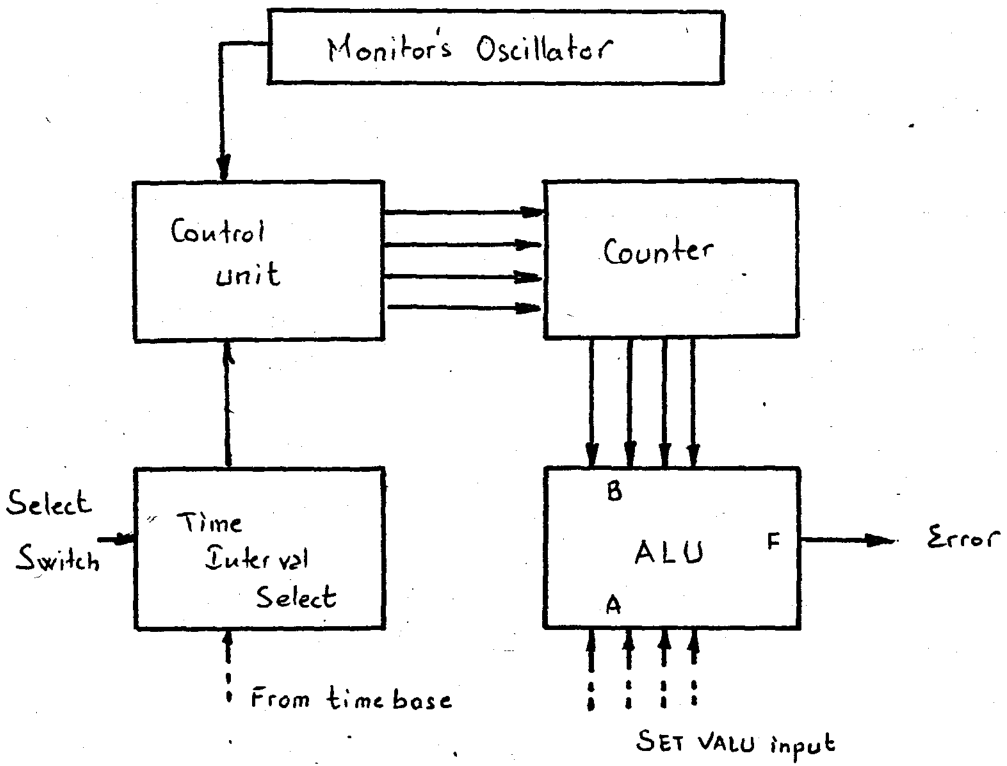

Fig.10

i- Counter, control, time base unit

This unit is based on the counting operation of the 74169 four bit presettable modulo 16, binary up/down counter, 7473 dual JK flip-flop, 74121 monostable multivibrator and 7475 four bit transparent latch were used in collaboration with 74169 for time interval select, generation of control signals and temporary memory purposes respectively. The circuit is shown in Fig. 12.

The functionning of this unit can be explained as fallows referring to the timing diagram.

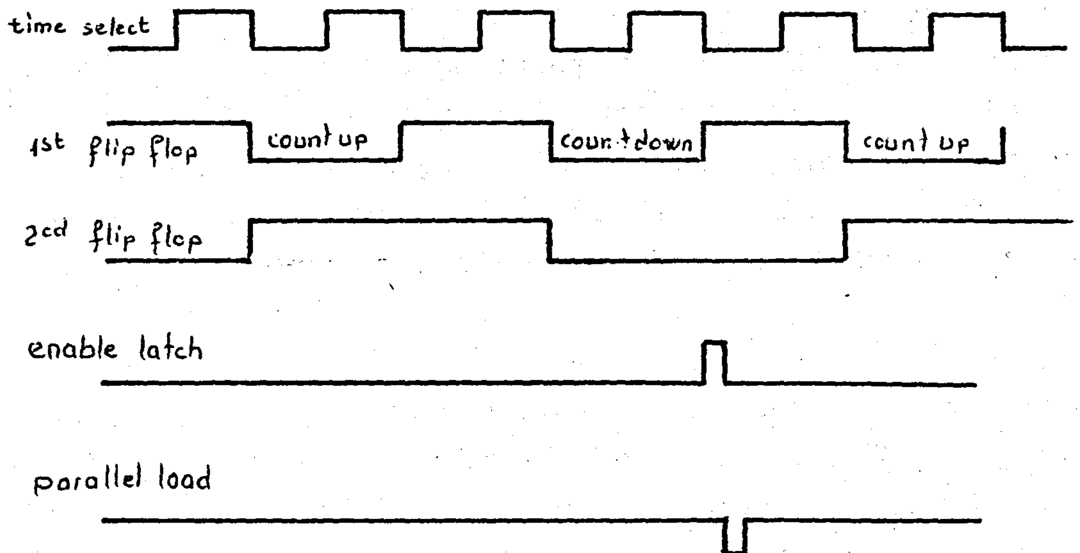

Fig.11 Timing

The 10 Hz signal received from the main time base is divided into 5 to get a 2 Hz signal. This furthermore is divided three times into 10 inorder to get 0.2, 0.02, 0.002 Hz signals. The required value is fed to the clock input of one of the JK flip-flops by selecting the necessary switch. This flip-flop functioning in toggle mode provides the count enable(CET) signal for the 74169. The second flip-flop cascades to the first, similarly provides count up/count down signal ($\overline{U}/\overline{D}$). The rising edge of the CET while U/$\overline{D}$ is low i.e. the down counting terminated triggers the first monostable multivibrator, 74121 producing a pulse in order to enable the latches, 7475's that will store the data (the difference in frequency for the selected time interval) temporarily.

The falling edge of this pulse, then triggers the second multivibrator, which produces the parallel load pulse for the 74169. This pulse permits the counter to take in the data present to its data pins. As all data pins are connected to ground 0.0.0.0 is inputted. This clears the contents of the counter and makes it ready for the next counting operation.

The terminal count pin (TC) of the least significant counter is connected to count enable (CEP) pin of the next significant counter. All binary counting is done on eight bit. In fact the individual count up and count down processes may require up to 2^{25}= 10 MHz, 25 bits because the counting frequency is in order of MHz but since we need the difference in frequency and this value is of the order of 0-255 Hz, 8 bit counting of least significant digits were enough for our purposes.

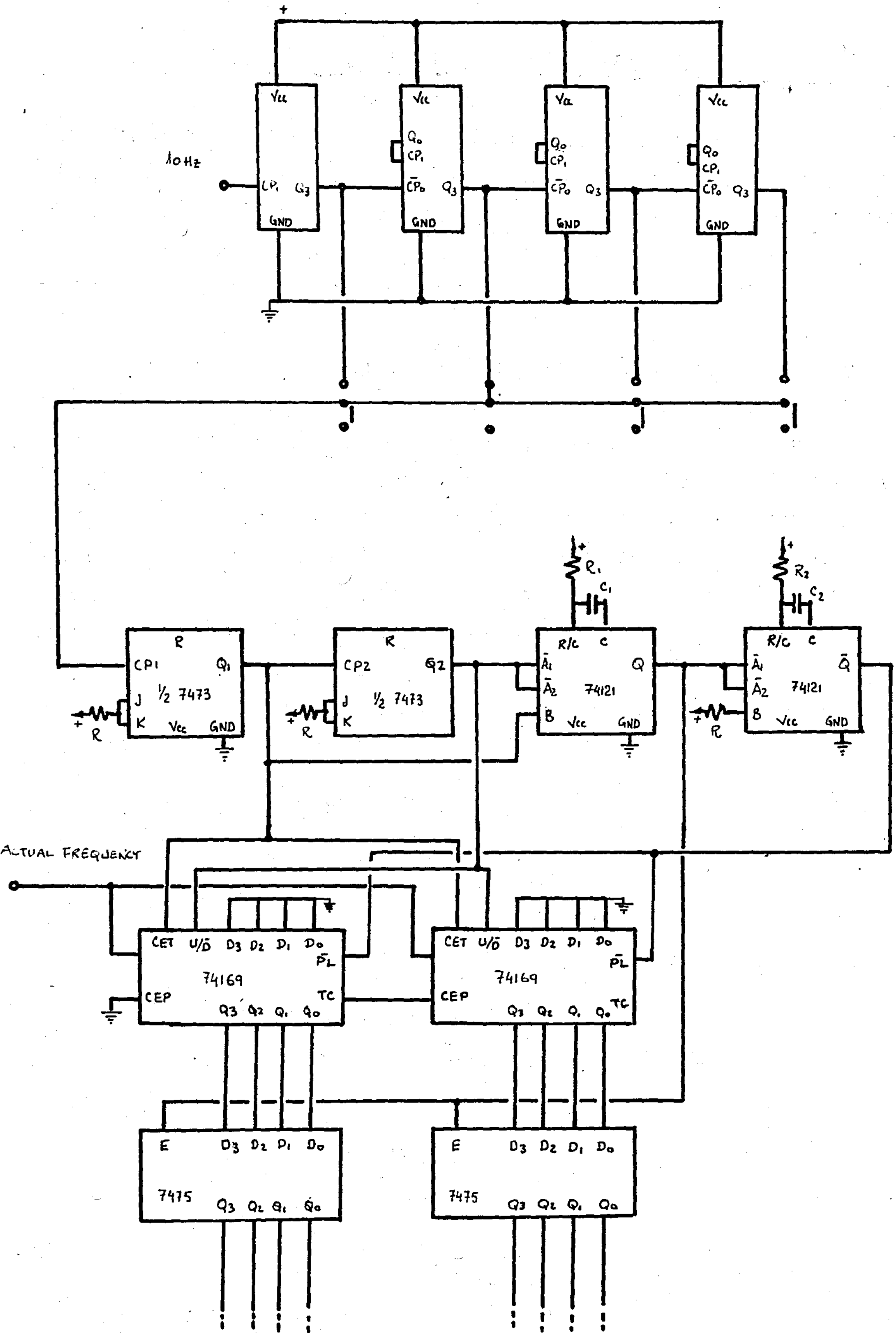

Fig.12 Time select control and counter unit

ii- Arithmetic Logic Unit and Error display

This unit is based on the 74181 ALU chip. Although this powerfull chip can do 16 arithmetic and 16 logic operations, it is used only for subtracting purposes. The required " rate of change of frequency " value is inputted to side A of ALU and the counted " actual rate of change of frequency" value is inputted to side B.

Selecting the chip in order to produce A minus B function by connecting low, high, high, low, low to $S_3S_2S_1S_0$ and M, function select and mode select inputs, respectively, we get the desired difference. This value actually is the deviation of the actual rate from the required rate. This eight bit error signal will then be used in the feedback loop of the rate controller, as well as it can be seen in binary form on the error display.

The connection of the ALU to outside world and to the counter is shown below.

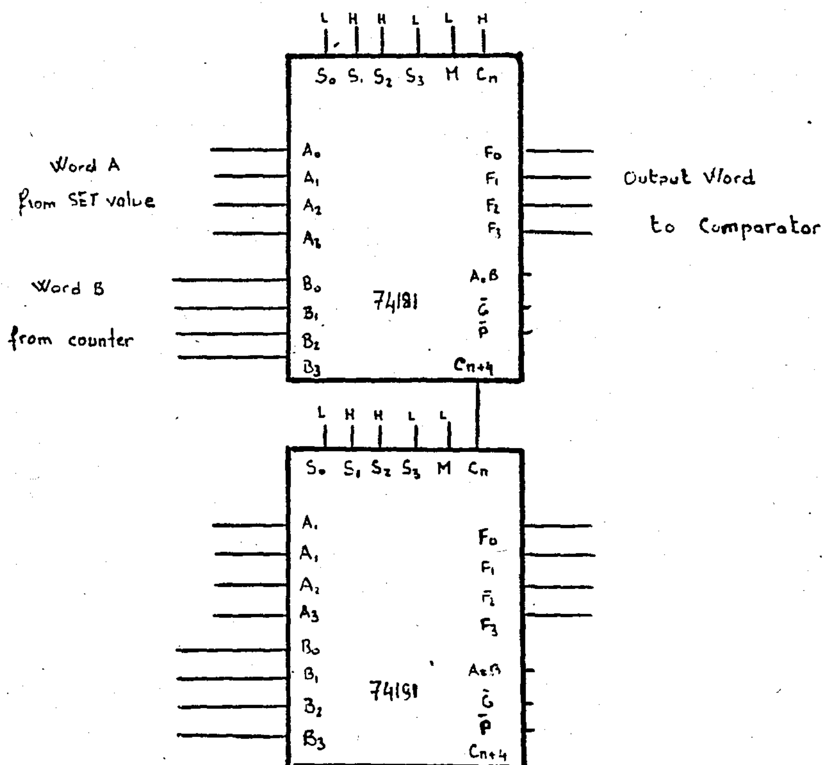

Fig. 13

B - PROPORTIONAL OR MICROPROCESSOR COMPATIBLE RATE CONTROL UNIT

The proportional or microprocessor compatible rate control unit is the feedback path of the evaporator. Either the error signal or the set value signal is fed to the comparator which decides the phase angle of the conducting part of the triac.

In proportional control mode the magnitude of the error directly drives the conduction angle. If the device is operating in external control or microprocessor control mode, the conduction angle is decided by the 8 bit digital set value input. If all bits are zero the evaporator will receive full current. If all bits are one the evaporator w'ont receive any current. If an accordingly programmed microprocessor of 8 bit output port could be connected to the set value input perfect control on power could be obtained.

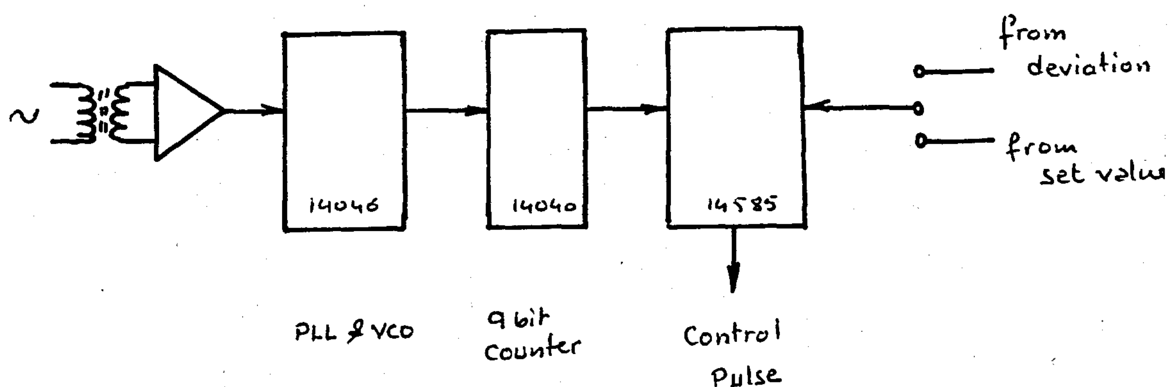

Fig.14

Fig.15

i- Phase Lock Loop(PLL) and VCO

The PLL consists of a phase comparator, a voltage controlled oscillator and a low pass filter, all arranged as shown in Fig.16

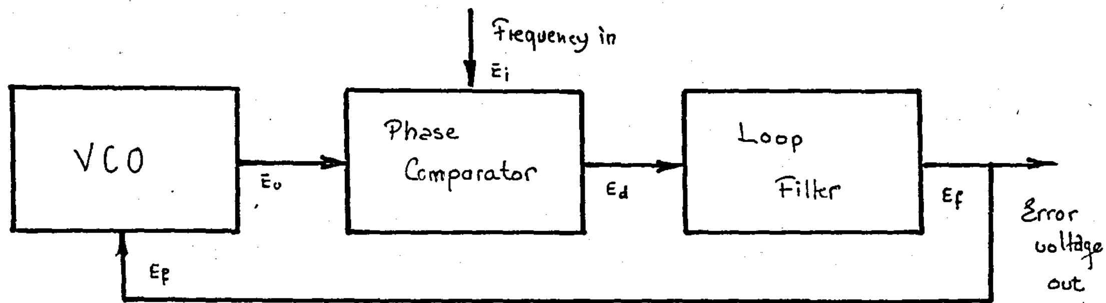

Fig.16

In operation, the VCO oscillates at a frequency determined by an external RC network. This frequency is applied to one input of the phase comparator. An external signal applied to the second input of the phase comparator causes it to generate an error voltage E_f, whose magnitude is proportional to the difference between the external source and VCO frequencies.

The low pass loop filter smooths the pulsating error voltage into a dc level which is then applied to the control input of the VCO. The VCO responds to the error voltage by mounting its frequency of oscillation toward that of the input signal. This capture process continues until the VCO frequency equals the input frequency. When this occurs, the PLL is said to be locked or phase is locked to the input signal.

When the PLL is locked to the input frequency, the VCO automatically tracks any changes in the input frequency that fall within a window called the lock range. The lock range is always greater than the capture range. The band frequencies over which the PLL can hunt for and capture an incoming signal.

Although the loop filter is essential for proper operation of the PLL, its time constant limits the speed with which the system can track changes in the input frequency. It also limits the capture range. On the other hand the loop filter helps prevent noise voltage from adversly affecting loop operation. The charge stored in the loop filter's capacitor helps the quick recapture of a signal temporarily lost because of noise spike or other transients.

Let θ_{in} be the phase angle of the input signal, and

θ_{vco} be the phase angle of the VCO output.

The phase of the VCO output being proportional to the error voltage with a proportionality constant k_{vco},

$$\theta_{vco} = k_{vco} \cdot E_f \qquad \text{(eq.1)}$$

The phase comparator itself producing an error voltage E_d proportional to the difference in phase with a proportionality constant k_{pc},

$$E_d = k_{pc} \cdot (\theta_{in} - \theta_{vco}) \qquad \text{(eq.2)}$$

Hence
$$\frac{\theta_{vco}(s)}{\theta_{in}(s)} = \frac{k_{vco} \cdot k_{pc} \cdot F(s)}{s + k_{vco} \cdot k_{pc} \cdot F(s)} \qquad \text{(eq.3)}$$

F(s) being the loop filter's transfer function for the simple RC, E_d 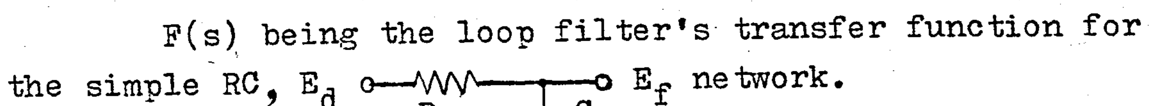 E_f network.

$$F(s) = \frac{E_f}{E_d} = \frac{1}{1 + s\tau_1} \qquad \text{(eq.4)}$$

where $\tau_1 = R_{1_{LP}} \cdot C_{LP}$

Therefore $$\frac{\theta_{vco}(s)}{\theta_{in}(s)} = \frac{k_{vco} \cdot k_{pc}/\tau_1}{s^2 + s/\tau_1 + k_{vco} \cdot k_{pc}/\tau_1} \quad \text{(eq. 5)}$$

hence the damping factor

$$\zeta = \tfrac{1}{2} \left(\frac{1}{k_{vco} \cdot k_{pc} \cdot \tau_1} \right)^{1/2} \quad \text{(eq. 6)}$$

and the natural frequencies

$$w_n = \left(\frac{k_{vco} \cdot k_{pc}}{\tau_1} \right)^{1/2} \quad \text{(eq. 7)}$$

From these equations we can see that large time constants reduce the damping factor and decrease the stability.

If the loop filter is improved by adding a damping resistor

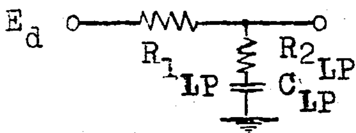

$$F(s) = \frac{E_f}{E_d} = \frac{s(\tau_1 + \tau_2)}{1 + s\,\tau_2} \quad \text{(eq. 8)}$$

$$\frac{\theta_{vco}(s)}{\theta_{in}(s)} = \frac{k_{vco} \cdot k_{pc}(\tau_1 + \tau_2) \cdot (1 + s\tau_2)}{s^2 + \left(\frac{1 + k_{vco} \cdot k_{pc} \cdot \tau_2}{(\tau_1 + \tau_2)} \right) \cdot s + \frac{k_{vco} \cdot k_{pc}}{(\tau_1 + \tau_2)}} \quad \text{(eq. 9)}$$

$$\zeta = \tfrac{1}{2} \left(\tau_2 + \frac{1}{k_{vco} \cdot k_{pc}} \right) \cdot \left(\frac{k_{vco} \cdot k_{pc}}{\tau_1 + \tau_2} \right)^{\frac{1}{2}} \quad \text{(eq. 10)}$$

$$w_n = \left(\frac{k_{vco} \cdot k_{pc}}{C_1 + C_2} \right)^{\frac{1}{2}} \quad \text{(eq. 11)}$$

Nominal values for $R1_{LP}$, $R2_{LP}$ and C_{LP} the elements of the LP filters are around 470K, 47K and 0.1 F respectively.

On the other hand the center frequency of the VCO is determined by the capasitor and one or two resistors. If only $R1_{vco}$ is used, the VCO frequency can be varied from 0Hz to a maximum frequency given by

$$f_{max} = \frac{1}{R1_{vco}(C1_{vco} + 32pF)} \qquad (eq.12)$$

Resistor $R2_{vco}$ is included when it is desirable to move the minimum frequency above 0Hz. The minimum frequency resulting from the inclusion of this offset resistor $R2_{vco}$ is given by

$$f_{min} = \frac{1}{R2_{vco}(C1_{vco} + 32pF)} \qquad (eq.13)$$

When $R2_{vco}$ is used the maximum VCO frequency is found by adding f_{min} to f_{max} of previous equation.

The output frequency of the VCO is requested to be 25600 Hz in order to drive the counter-dividing circuit. If 50 Hz signal is taken in as input to PLL, the 9 bit counter dividing 25600 Hz to $2^9 = 512$ will produce a 50 Hz signal that will be in phase with the input signal.

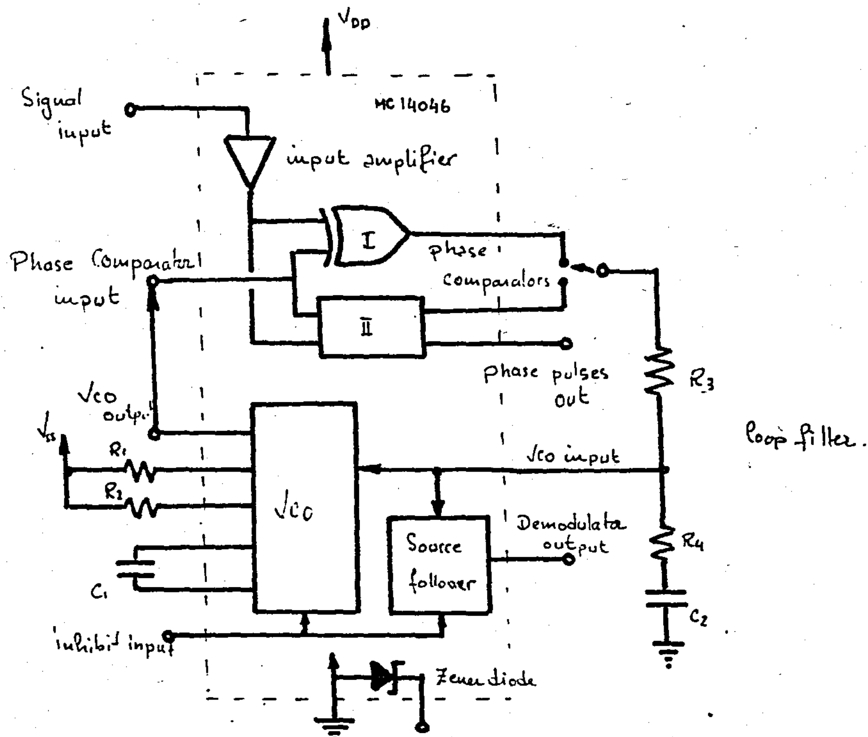

Fig.17

In addition the input signal, i.e. 50 Hz. mains supply is fed to PLL through a comparator LM741 which detects the zero crossings of the mains-sine wave and produce a square wave; as shown in Fig.18.

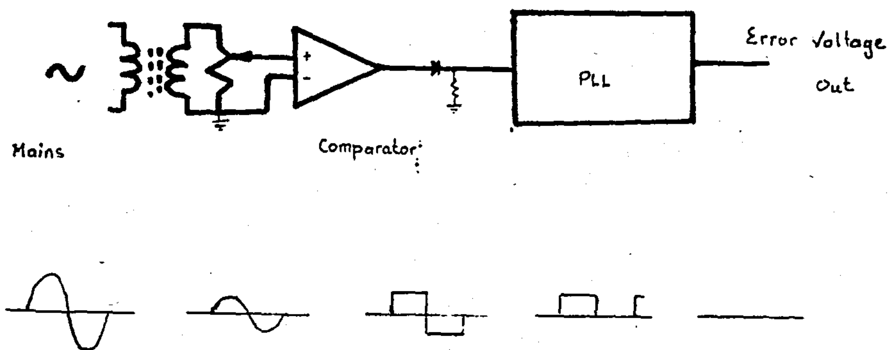

Fig.18

ii- Counter unit

As the main purpose of using PLL is to keep control over the phase even if the mains frequency changes the idea will be able to find its true value only when the 512 steps of the counter falls exactly within one period of the mains supply.

14040, 12 bit counter is used in order to produce the 512 steps. The VCO output providing 25600 Hz. when the mains frequency is 50 Hz. drives the count input of the counter. As within one period of the mains there falls 512 steps, the resolution .i.e. the minimum interval that can be differentiated from another is of an angle of 0.7°.

$$R = \frac{360}{512} = 0.7^{\circ} \text{ per step.}$$

If a resolution different than 0.7° per step is required, the VCO center frequency can be adjusted accordingly. 256 or 1024 steps within one period will require 12800 or 51200 Hz. respectively yielding a resolution of 1.4° or 0.35° per step.

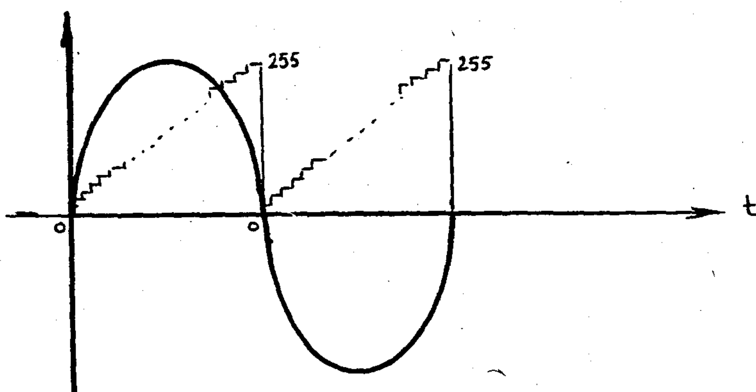

Fig.19

If the 25600 Hz clock signal was not received from the VCO in connection with PLL but from another constant source, the variation in the mains frequency will produce some dis-

orders as shown in the Fig.20.

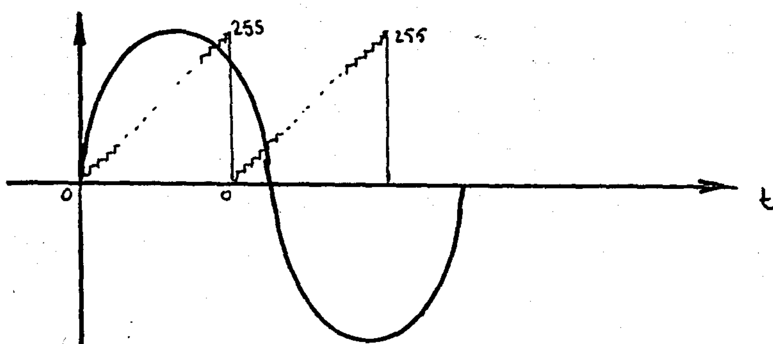

Fig.20

We can explain this process as fallows:

Assuming that the mains frequency has falled to 45 Hz the duration of the half cycle will be now 11.1 msec., while it was exactly 10.1 msec. for 50 Hz. For this 1.1 msec extra time interval the counter still will continue to count and will go out of its range of 256 units per half cycle. To correct this, the count pulses to the counter input should have now a frequency of 23040 Hz instead of 25600 Hz, so that the latter can count only 256 steps within the new period.

The MC14040, 12 bit counter unit is shown in Fig.21. The unused Q_9, Q_{10}, Q_{11} outputs are left open.

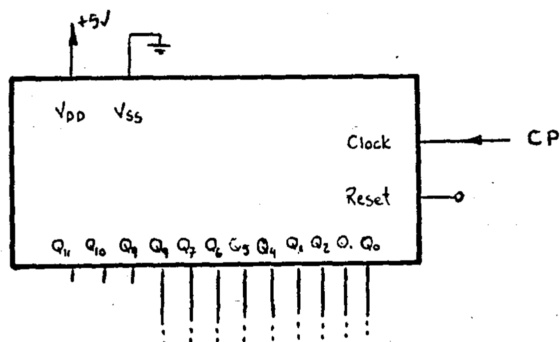

Fig.21

iii- The comparator

The error signal obtained from the arithmetic logic unit by taking the difference of the actual " rate of change in frequency" and the required value forms one of the inputs to the comparator. The other input to the comparator is provided through the phase locked loop and eight bit counter. The control action is directly proportional to the error signal.

The comparator chip is the MC14585. Two of them is used in order to get eight bit of data comparison. The output of the comparator being in less than, equal, greater than form, the equal or greater than output is used. This signal is fed to SCR triggering circuit.

As seen in Fig.22 an output pulse is obtained from the comparator for each half cycle of the main supply. The delay of this pulse is directly related to the error signal.

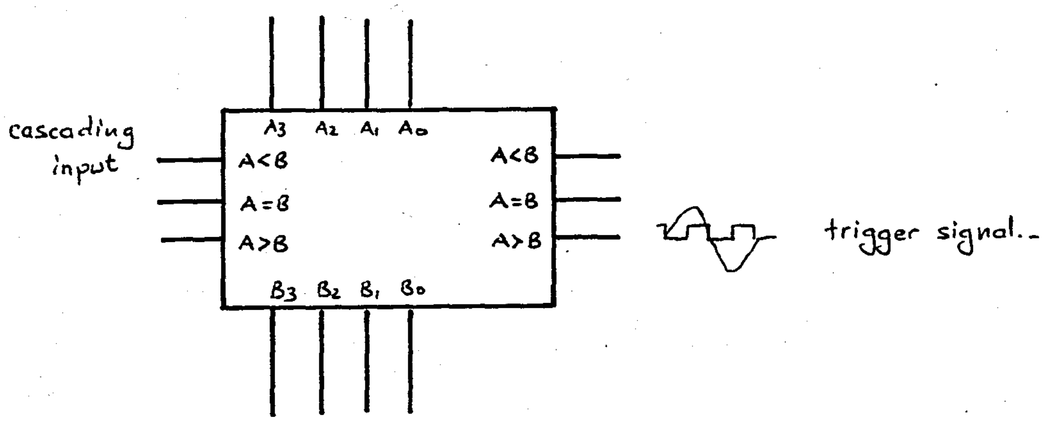

Fig.22

iv- SCR trigger unit

The power that will be fed to the evaporator is controlled by this unit. The comparator output signal determines the triggering instant of the triac.

As shown in Fig.23 below the comparator output provides sufficient current to the opto coupler. The photo transistor within the opto coupler will in turn cause the darlington transistor point to turn off, so that very little current flows through the bridge circuit. In effect the bridge circuit no longer forms a "short" between points A& B, so that voltage between these points can rise above the zener voltage determined by D5 and D6. Depending on the phase of the mains voltage, one of these diodes will be forwared biased. The triac now will receive gate current, so it turns on switching on the load. If the LED in the opto coupler is not driven, the photo transistor will turn off. As the voltage between points A and B rises after a zero crossing of the mains, T1 will now turn on. This limits the voltage to two diode drops, two base emitter drops and saturation voltage of T1; 3 volts in all. Therefore the zeners can not conduct, the load is switched off.

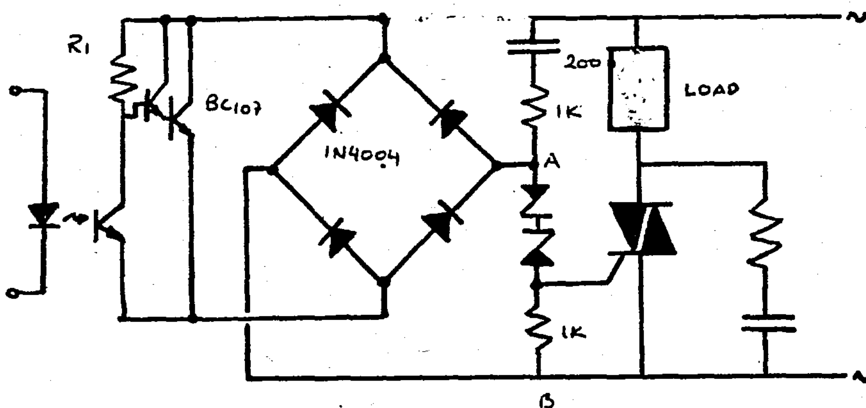

Fig.23 Triac trigger unit

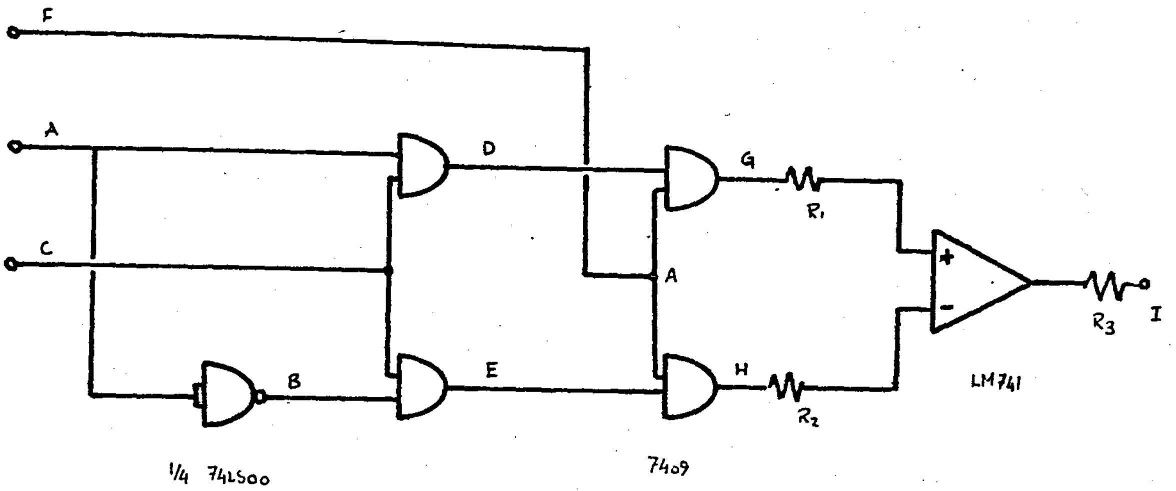

Fig. 24

SCR triggering waveform generation

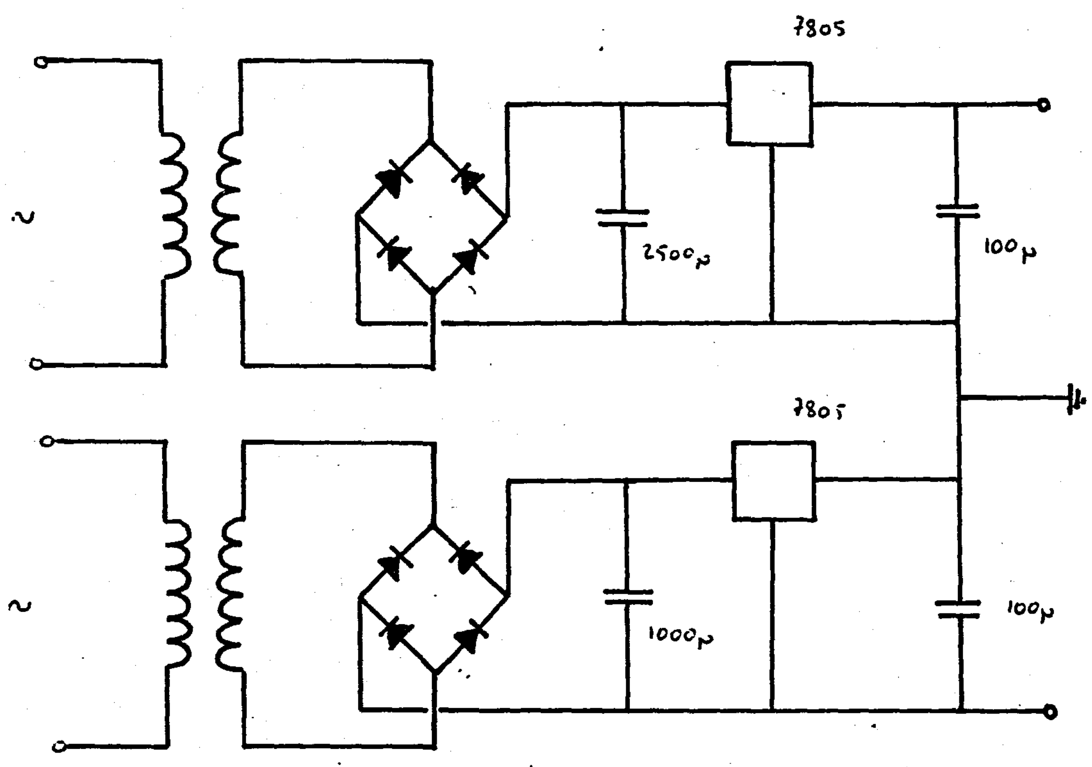

POWER SUPPLY UNIT.

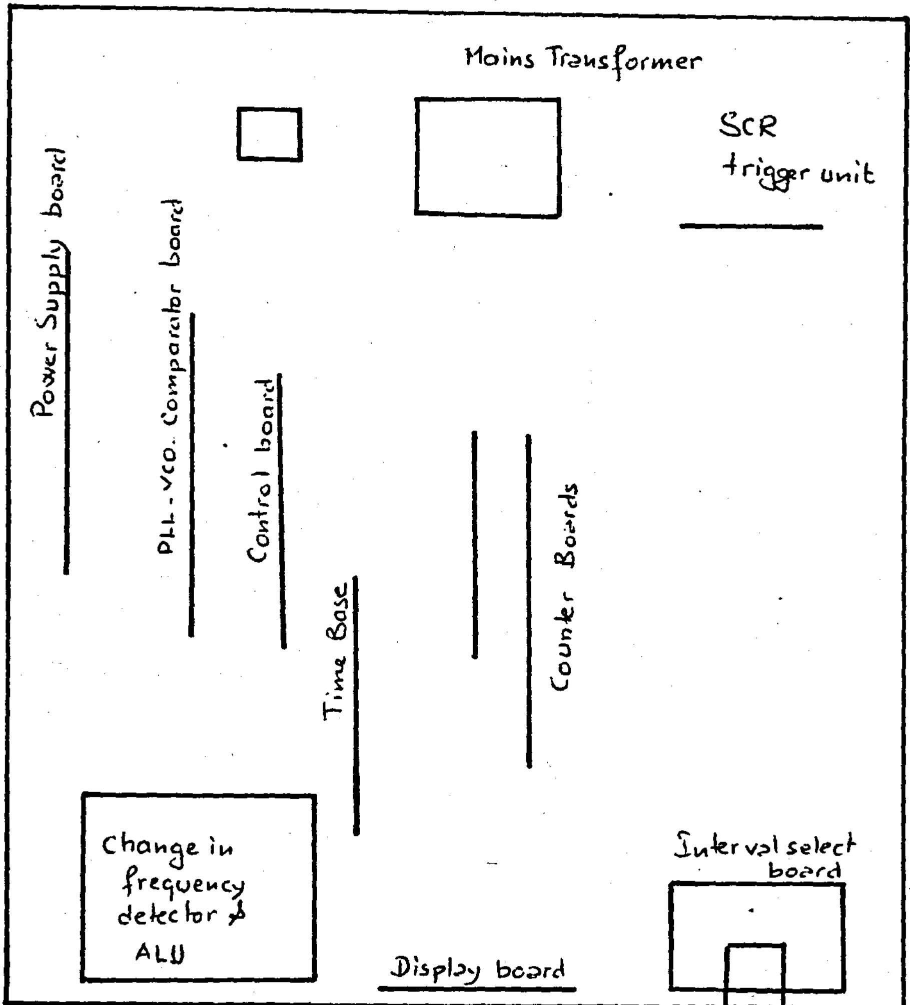

Top wiev

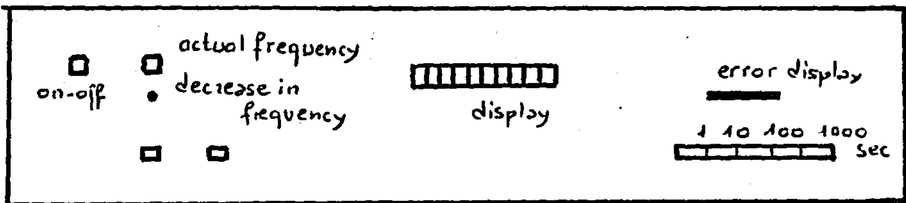

Front Panel

GENERAL CONFIGURATION OF THE SYSTEM.

LIST OF REFERANCES

(1) HOLLAND.L.,"Vacuum Deposition of Thin Films". John Wiley & Sons INC., New York, 1961.

(2) Steckelmacher, W., in L.Holland (ed), "Thin Film Micro-electronics", John Wiley & Sons INC., New York, 1965.

(3) Behrndt, K.H. in G.Hass and R.E.Thun (eds). "Physics of Thin Films" Vol.3, Academic Press INC., New York,1966.

(4) Poulis.J.A, P.J.Meeusen, W.Dekker and J.P. de Mey, in "Vacuum Microbalance Techniques" Vol.6, Plenum Press, New York, 1967.

(5) Sauerbrey, G.Phys.Verhandl, 8, 113 (1957).

(6) Sauerbrey, G.Z.Physik, 155, 206 (1959).

(7) Lostis, M.P., J.Phys.Radium, 20,25 (1959).

(8) Phelps, F.F., Proc 11th Ann.Symp.Frequency Control, Forth Monmounth, N.J., 1957, pp.256.

(9) Stockbridge, C.D., in "Vacuum Microbalance Techniques", Vol.5, Plenum Press, New York, 1966, pp.193.

(10) Eschbach, H.L., and E.W.Kruidhof, in "Vacuum Microbalance Techniques" Vol.5, Plenum Press., New York, 1966.

(11) Pulker, H.K., Z.Angew, Phys.20, 537, 1966.

(12) Pulker, H.K., and W.Schaedler, Ext.Abstr.14th AVS Symp. 1967, Herbick and Held Printing Co., Pittsburgh, Pa.

(13) Berndt, K.H., and R.W.Love, Vacuum, 12, 1962.

(14) Reinhard Glang.,"Handbook of Thin Film Technology", Mac. Graw Hill, New York,1970.

(15) Robinson C.J., and Baker M.A., J.Phys.E: Scientific Instrum. Vol.11, 1978, pp.625.

(16) Balasubramanian and Riesz R.P., Rev.Sci.Instrum., 52(5), 1981, pp.746.

(17) Kocagöz, N.,"An Analog Thin Film Thickness Monitor", Thesis, B.U., 1980.

(18) Heyman J.S. and Miller W.E., J.Vac.Sci.Technol.15(2), 1978 ,pp.219.

(19) Chih-Shun.Lu, "J.Appl.Phys.", Vol. 43, 1972, pp.4385.

(20) Thomas, H.E., "Handbook of Integrated Circuits", Prentice Hall Inc., New York, 1971.

(21) Schwartz, S., "Integrated Circuit Technology", Mac Graw Hill,New York, 1967.

(22) Heavens, O.S., "Thin Film Physics", Methuen & Co.Ltd., 1970.

(23) Le Comber, P.G. and Mort J., "Electronic and Structural Properties of Amorphous Semiconductors", Academic Press, London, 1973.

(24) Tobey,Greame, Huelsman, "Operational Amplifiers", Mac Graw Hill, 1971.

(25) Chute M., Chute D.R., "Electronics in Industry", Mc.Graw Hill, Kogakusha, 1979.

(26) Taub.H., Schilling.D., "Digital Integrated Electronics", Mc.Graw Hill, Kogakus a, 1977.

(27) Tocci.R.J., "Digital Systems", Prentice Hall International, London, 1980.

(28) Data Sheets of Motorola and National Semiconductors.

(29) Forest.M.M., Popular Electronics, 7. 1980.

(30) HOAND.L.H., Proceedings of the IEEE, Vol.66, 1978, pp.90.

(31) DRISCOLL, COUGHLIN, "Solid State Devices and Applications" Prentice Hall, London, 1975.

(32) Holland, Steckelmacher, Yarwood, "Vacuum Manual", SPON, London, 1974.

MANUFACTURER:	Airco Temescal	Balzers	Edwards High Vacuum		Kronos
Model no.	DTM-321	QSG201	FTM2	FTM2D	QM300 series
Model number of crystal	SHO-321	QSK 211, 181, 221, 113, 114			FTT 4, 5, 6
Range					
Total frequency shift	1 MHz	0–30 kHz			
Number of ranges	2	6	10	4	3
Frequency shift to produce FSD for each			calibrated in Å, 100, 300, 1000, 3000, 10 000 for densities 1 to 10 g/cm^3		
Sensitivity: frequency shift per μg loading					
Stability: frequency shift per hour		5 Hz			
Accuracy	0·05%		± 2% FSD		± 0·1% of full scale plus resolution
Output indication	Digital		Meter	Digital	Analogue or digital
Output signal		10 mV to recorder	0–5 V	0–5 V	A: 0–5 V D: Buffered 5 V four digit parallel 8421 BCD code
Ancillary units			UHV crystal holder, additional oscillator, process terminator, source current stabilizer		

MANUFACTURER:	Sloan		Ultek	Varian	
Model no.	200	DTM-4	DDM	985-7001, to 985-7013	988-0900
Model number of crystal			Monoprobe	985-7150, 985-7151, 985-7152	988-0907
Range					
Total frequency shift		0–100 kHz		1 mHz	0–300 kHz
Number of ranges	3	5		3	6
Frequency shift to produce FSD for each				Calibrated in k Å 10 100, 1000	1, 3, 10, 30, 100, 300 kHz
Sensitivity: frequency shift per μg loading					20 Hz
Stability: frequency shift per hour				8 Hz	1 x 10^{-5}
Accuracy		± 2% FS		0·01%	± 2%
Output indication			Digital	Digital	Linear
Output signal	Recorder 0–5 V	Recorder 0–4·5 V		0–10 V	
Ancillary units	Remote crystal holder, perforated optic transmission shields, DDS digital dial set point			Rate controller programmer	

Note: 1 Å = 0·1 nm; 1 kÅ = 100 nm = 0·1 μm.

2.2.12 Rate meters

MANUFACTURER:	Airco Temescal	Balzers	Edwards High Vacuum	Electrotech
Model no.	DPC-333	QRG 201A	Deposition ratemaster	P1401
Associated thickness monitor model number	DTM321	QSG 201	FTM2, FTM2D	P1001
Ranges			3; 0–0·3, 0–1, 0–3%/s of selected thickness down to 0·005 Å/s	
Output signals	0–10 V	10 mV–100 mV recorder connections		0–10 V
Ancillary units	PCM341 Multi-material programmer			Programmable power supply P2101 for evaporation source

MANUFACTURER:	Kronos		Sloan	Ultek
Model no.	RI100	RO200	DRC	DDM
Associated thickness monitor model number	QM300 or ADS200	QM300 or ADS200	DTM4	
Ranges	3, 0–20, 0–200, 0–2000, Å/s	3, 0–20, 0–200, 0–2000 Å/s	10–300 Hz/s	
Output signals	Analogue 0-5 V	Analogue 0-5 V	0–9 V recorder	
Ancillary units				

MANUFACTURER:	Varian	
Model no.	985-7014	988-0901
Associated thickness monitor model number	985-7001 to 985-7009, 985-7011	988-0900
Ranges	0·0001, 0·1, 1, 10% FSD	18 ranges, 10,000 Hz/s
Output signals	0– –10 V	0––9 V, 0––100 mV
Ancillary units	Programmer	Deposition controller, signal amplifier

Note: 1 Å = 0·1 nm; 1 kÅ = 100 nm = 0·1 μm.